arXiv:1706.02507v2 [physics.flu-dyn] 2 Aug 2017

Wave Scattering in Spatially Inhomogeneous Currents

Semyon Churilov

Institute of Solar-Terrestrial Physics of the Siberian Branch of Russian Academy of Sciences, Irkutsk-33, PO Box 291, 664033, Russia.

Andrei Ermakov

School of Agricultural, Computational and Environmental Sciences, University of Southern Queensland, QLD 4350, Australia.

Yury Stepanyants*

Department of Applied Mathematics, Nizhny Novgorod State Technical University, Nizhny Novgorod, 603950, Russia and

School of Agricultural, Computational and Environmental Sciences, University of Southern Queensland, QLD 4350, Australia.

(Dated: March 4, 2022)

We analytically study a scattering of long linear surface waves on stationary currents in a duct (canal) of constant depth and variable width. It is assumed that the background velocity linearly increases or decreases with the longitudinal coordinate due to the gradual variation of duct width. Such a model admits analytical solution of the problem in hand, and we calculate the scattering coefficients as functions of incident wave frequency for all possible cases of sub-, super, and trans-critical currents. For completeness we study both co-current and counter-current wave propagation in accelerating and decelerating currents. The results obtained are analysed in application to recent analog gravity experiments and shed light on the problem of hydrodynamic modelling of Hawking radiation. The paper is published in Physical Review D.

* Corresponding author: Yury.Stepanyants@usq.edu.au

I. INTRODUCTION

Since 1981 when Unruh established the analogy in wave transformation occurring at the horizon of a black hole and at a critical point of a hydrodynamic flow [1] there have been many attempts to calculate the transformation coefficients and find the analytical expression for the excitation coefficient of a negative energy mode (see, for instance, [2–5] and references therein). In parallel with theoretical study there were several attempts to model the wave scattering in spatially inhomogeneous currents experimentally and determine this coefficient through the measurement data [6, 7] (similar experiments were performed or suggested in other media, for example, in the atomic Bose-Einstein condensate – see [8] and numerous references therein). In particular, the dependence of amplitude of a negative energy mode on frequency of incident wave in a water tank was determined experimentally [6]; however several aspects of the results obtained in this paper were subject to criticism.

The problem of water wave transformation in spatially inhomogeneous currents is of significant interest itself and there is a vast number of publications devoted to theoretical and experimental study of this problem. However in applying to the modelling of Hawking's effect, the majority of these publications suffer a drawback which is related to the parasitic effect of dispersion, whereas the dispersion is absent in the pure gravitational Hawking effect.

Below we consider a model which describes a propagation of small-amplitude long surface water waves in a duct (canal) of constant depth but variable width. The dispersion is absent, and the model is relevant to the analytical study of the Hawking effect. We show that the transformation coefficients can be found in the exact analytical forms both for co-current and counter-current wave propagation in gradually accelerating and decelerating currents.

We believe that the results obtained can be of wider interest, not only as a model of Hawking's effect, but in application to real physical phenomena occurring in currents in non-homogenous ducts, at least at relatively small Froude numbers. We consider all possible configurations of the background current and incident wave. The paper's contents is presented below.

CONTENTS

I. Introduction 2

II. Derivation of the Governing Equation 4

III. Qualitative Analysis of the Problem Based on the JWKB Approximation 7

IV. Wave Scattering in Inhomogeneous Currents With a Piece-Linear Velocity Profile 10

A. Wave transformation in sub-critical currents 11

1. Accelerating currents. Transformation of downstream propagating incident wave 12

2. Accelerating currents. Transformation of upstream propagating incident wave 14

3. Wave transformation in a decelerating sub-critical current 17

B. Wave transformation in a super-critical current 17

1. Transformation of a positive-energy wave in an accelerating current 19

2. Transformation of negative-energy wave in an accelerating current 22

3. Wave transformation in a decelerating super-critical current 24

C. Wave transformation in trans-critical accelerating currents $0 < V_1 < 1 < V_2$ 25

D. Wave transformation in trans-critical decelerating currents $V_1 > 1 > V_2 > 0$ 30

1. Transformation of downstream propagating positive-energy wave 33

2. Transformation of downstream propagating negative-energy wave 36

3. Transformation of a counter-current propagating wave 37

V. Discussion and Conclusion 39

Acknowledgments 44

A. Energy Flux Conservation 44

B. Derivation of Matching Conditions for Equation (8) 46

C. The Transformation Coefficients in the Long-Wave Limit 47

References 48

II. DERIVATION OF THE GOVERNING EQUATION

Let us consider the set of equations for water waves on the surface of a perfect fluid of a constant density ρ and depth h. Assume that the water moves along the x-axis with a stationary velocity $U(x)$ which can be either an increasing or a decreasing function of x. Physically such a current can be thought as a model of water flow in a horizontal duct with a properly varying width $b(x)$. We will bear in mind such a model, although we do not pretend here to consider a current in a real duct, but rather to investigate an idealized hydrodynamic model which is described by the equation analogous to that appearing in the context of black hole evaporation due to Hocking radiation [1–5, 9–11].

In contrast to other papers also dealing with the surface waves on a spatially varying current (see, e.g., [2–5]), we consider here the case of shallow-water waves when there is no dispersion, assuming that the wavelengths $\lambda \gg h$.

In the hydrostatic approximation, which is relevant to long waves in shallow water [12], the pressure can be presented in the form $p = p_0 + \rho g(\eta - z)$, where p_0 is the atmospheric pressure, g is the acceleration due to gravity, z is the vertical coordinate, and $\eta(x,t)$ is the perturbation of free surface ($-h \leq z \leq \eta$). Then the linearized Euler equation for small perturbations having also only one velocity component $u(x,t)$ takes the form:

$$\frac{\partial u}{\partial t} + \frac{\partial (Uu)}{\partial x} = -g\frac{\partial \eta}{\partial x}. \tag{1}$$

The second equation is the continuity equation which is equivalent to the mass conservation equation for shallow-water waves:

$$\frac{\partial S}{\partial t} + \frac{\partial}{\partial x}\left[S\left(U+u\right)\right] = 0, \tag{2}$$

where $S(x,t)$ is the portion of the cross-section of a duct occupied by water, $S(x,t) = b(x)[h + \eta(x,t)]$, where $b(x)$ is the width of the duct.

For the background current Eq. (2) gives the mass flux conservation $Q \equiv \rho\, U(x)S(x) = \rho\, U(x)b(x)h = \text{const}$. Inasmuch as $h = \text{const}$, we have $U(x)b(x) = Q/\rho h = \text{const}$, and Eq. (2) in the linear approximation reduces to:

$$b(x)\frac{\partial \eta}{\partial t} + \frac{\partial}{\partial x}\left[b(x)\left(U\eta + uh\right)\right] = 0. \tag{3}$$

Thus, the complete set of equations for shallow water waves in a duct of a variable width consists of Eqs. (1) and (3). This set can be reduced to one equation of the second order.

To this end let us divide first Eq. (3) by $b(x)$ and rewrite it in the equivalent form:

$$\frac{\partial \eta}{\partial t} + U\frac{\partial \eta}{\partial x} = -hU\frac{\partial}{\partial x}\frac{u}{U}. \tag{4}$$

Expressing now the velocity component u in terms of the velocity potential φ, $u = \partial\varphi/\partial x$, and combining Eqs. (1) and (4), we derive

$$\left(\frac{\partial}{\partial t} + U\frac{\partial}{\partial x}\right)\left(\frac{\partial \varphi}{\partial t} + U\frac{\partial \varphi}{\partial x}\right) = c_0^2 U\frac{\partial}{\partial x}\left(\frac{1}{U}\frac{\partial \varphi}{\partial x}\right), \tag{5}$$

where $c_0 = \sqrt{gh}$ is the speed of linear long waves in shallow water without a background current.

As this equation describes wave propagation on the stationary moving current of perfect fluid, it provides the law of wave energy conservation which can be presented in the form (its derivation is given in Appendix A):

$$\frac{\partial \mathcal{E}}{\partial t} + \frac{\partial J}{\partial x} = 0, \tag{6}$$

where

$$\mathcal{E} = \frac{\mathrm{i}}{U}\left[\overline{\varphi}\left(\frac{\partial \varphi}{\partial t} + U\frac{\partial \varphi}{\partial x}\right) - \varphi\left(\frac{\partial \overline{\varphi}}{\partial t} + U\frac{\partial \overline{\varphi}}{\partial x}\right)\right], \quad J = \mathcal{E}U - \frac{\mathrm{i}\,c_0^2}{U}\left(\overline{\varphi}\frac{\partial \varphi}{\partial x} - \varphi\frac{\partial \overline{\varphi}}{\partial x}\right),$$

and the over-bar denotes complex conjugation.

Solution of the linear equation (5) can be sought in the form $\varphi(x,t) = \Phi(x)\mathrm{e}^{-\mathrm{i}\,\omega t}$, then it reduces to the ODE for the function $\Phi(x)$:

$$\left(-\mathrm{i}\,\omega + U\frac{d}{dx}\right)\left(-\mathrm{i}\,\omega\Phi + U\frac{d\Phi}{dx}\right) = c_0^2 U\frac{d}{dx}\left(\frac{1}{U}\frac{d\Phi}{dx}\right). \tag{7}$$

If we normalize the variables such that $U/c_0 = V$, $x/L = \xi$, and $\omega L/c_0 = \hat{\omega}$, where L is the characteristic spatial scale of the basic current, then we can present the main equation in the final form:

$$V\left(1 - V^2\right)\frac{d^2\Phi}{d\xi^2} - \left[\left(1 + V^2\right)V' - 2\,\mathrm{i}\,\hat{\omega}V^2\right]\frac{d\Phi}{d\xi} + V\hat{\omega}^2\Phi = 0, \tag{8}$$

where the prime stands for here and below differentiation with respect to the entire function argument (in this particular case with respect to ξ).

If the perturbations are monochromatic in time, as above, then the wave energy $\mathcal{E}$ and energy flux J do not depend on time, therefore, as follows from Eq. (6), the energy flux does not depend on x too, so $J = \mathrm{const}$.

For the concrete calculations we chose the piece-linear velocity profile, assuming that the current varies linearly within a finite interval of x and remains constant out of this interval (see Fig. 1):

$$V_a(\xi) = \begin{cases} V_1 \equiv \xi_1, & \xi \le \xi_1, \\ \xi, & 0 < \xi_1 < \xi < \xi_2, \\ V_2 \equiv \xi_2, & \xi \ge \xi_2; \end{cases} \qquad V_d(\xi) = \begin{cases} V_1 \equiv -\xi_1, & \xi \le \xi_1, \\ -\xi, & \xi_1 < \xi < \xi_2 < 0, \\ V_2 \equiv -\xi_2, & \xi \ge \xi_2, \end{cases} \tag{9}$$

where $V_a(\xi)$ pertains to the accelerating current, and $V_d(\xi)$ – to the decelerating current. To simplify further calculations, we have chosen, without the loss of generality, the origin of the coordinate frame such that the velocity profile is directly proportional to $\pm\xi$ in the interval $\xi_1 \le \xi \le \xi_2$ as shown in Fig. 1). For such velocity configurations it is convenient to set $L = (x_2 - x_1)c_0/(U_2 - U_1) = (x_2 - x_1)/|V_2 - V_1|$.

The choice of piece-linear velocity profile allows us to reduce the governing equation (8) to the analytically solvable equation and obtain exact solutions. The corresponding water flow can be realized in a duct with a variable width, which is constant, $b = b_1$, when $\xi \le \xi_1$, then gradually varies along the ξ-axis as $b(\xi) = b_1\xi_1/\xi$ in the interval $\xi_1 \le \xi \le \xi_2$, and after that remains constant again, $b_2 = b_1\xi_1/\xi_2$ when $\xi \ge \xi_2$. Schematically the sketch of a duct with gradually decreasing width that provides an accelerating current is shown in Fig. 2.

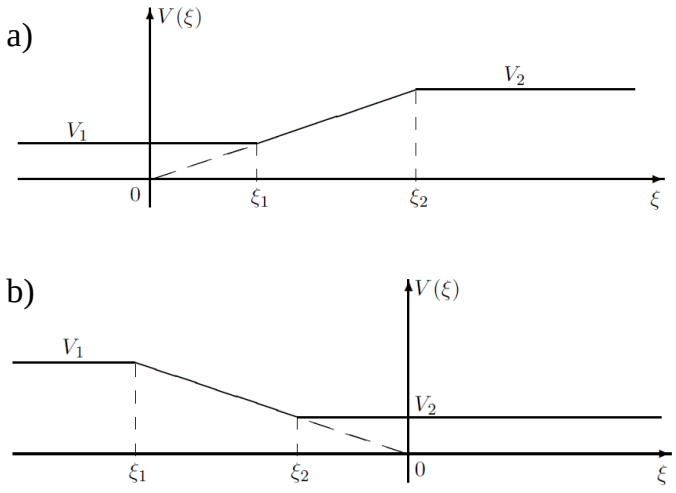


FIG. 1. Sketch of accelerating (a) and decelerating (b) background currents.

Equation (8) should be augmented by the boundary conditions at $\xi \to \pm\infty$ which specify the scattering problem, as well as by the matching conditions at $\xi = \xi_1$ and $\xi = \xi_2$. The

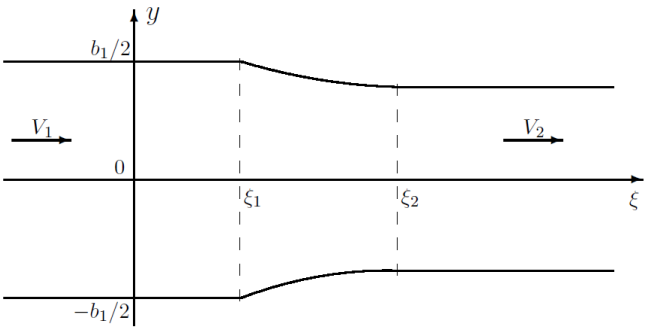


FIG. 2. The sketch of a duct with the decreasing width that provides spatially accelerating background current.

latter conditions reduce to the continuity of the function $\Phi(\xi)$ and its derivative $\Phi'(\xi)$ (see Appendix B for the derivation):

$$\Phi(\xi_{1,2}+0)=\Phi(\xi_{1,2}-0), \qquad \Phi'(\xi_{1,2}+0)=\Phi'(\xi_{1,2}-0). \tag{10}$$

On the basis of Eq. (8) and matching conditions (10), we are able to study analytically all possible cases of orientation of an incident wave and a current, assuming that the current can be sub-critical ($V_{1,2}<1$), trans-critical ($V_1>1$, $V_2<1$ or vice versa $V_1<1$, $V_2>1$), or super-critical ($V_{1,2}>1$).

III. QUALITATIVE ANALYSIS OF THE PROBLEM BASED ON THE JWKB APPROXIMATION

Before the construction of an exact solution for wave scattering in currents with the piece-linear velocity profiles, it seems reasonable to consider the problem qualitatively to reveal its specific features which will help in the interpretation of results obtained.

Consider first a long sinusoidal wave propagating on a current with constant U. Assume, in accordance with the shallow-water approximation, that the wavelength $\lambda \gg h$. The dispersion relation for such waves is

$$(\omega-\mathbf{kU})^2=c_0^2k^2, \tag{11}$$

where $\mathbf{k}=(k,0,0)$ is a wave vector related with a wavelength $\lambda=2\pi/|\mathbf{k}|$.

A graphic of the dispersion relation is shown in Fig. 3 for two values of the current speed, sub-critical, $U<c_0$, and super-critical, $U>c_0$. Since we consider dispersionless shallow-water waves, graphics of the dependences $\omega(k)$ are straight lines formally extending from

minus to plus infinity. We suppose, however, that the frequency ω is a non-negative quantity which is inversely proportional to the wave period; therefore, without loss of generality, we can ignore those portions of dispersion lines which correspond to negative frequencies (in Fig. 3 they are shown by inclined dashed lines). The dashed horizontal line in Fig. 3 shows a particular fixed frequency of all waves participating in the scattering process.

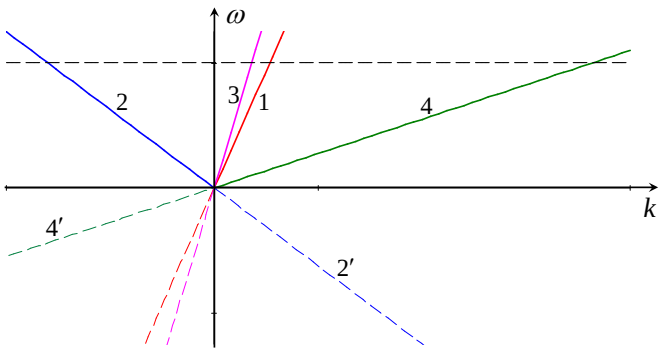


FIG. 3. (color online) The dispersion dependences for surface waves on uniformly moving shallow water. Lines 1 and 2 pertain to co-current and counter-current propagating waves respectively in a sub-critical current ($U < c_0$). Lines 3 and 4 pertain to positive- and negative-energy waves respectively in a super-critical current ($U > c_0$) both propagating downstream.

For co-current propagating waves with $\boldsymbol{k} \uparrow\uparrow \mathbf{U}$ the dispersion relation (11) reduces to $\omega = (U + c_0)|\mathbf{k}|$, whereas for counter-current propagating waves with $\boldsymbol{k} \downarrow\uparrow \mathbf{U}$ it is $\omega = |U - c_0||\mathbf{k}|$. Thus, the dispersion lines for surface waves on a current are not symmetrical with respect to the vertical axis $k = 0$. When the current speed U increases, the right branch 1 turns toward the vertical axis (cf. lines 1 and 3 in Fig. 3). The left branch 2 in this case tilts toward the negative half-axis k; coincides with it when $U = c_0$, and then, when $U > c_0$, it goes to the lower half-plane and becomes negative. However, its negative portion $2'$ goes up, passes through the axis k and appears in the upper half-plane as the dispersion line 4. Thus, waves corresponding to lines 3 and 4 are downstream propagating waves, whereas there are no upstream propagating waves, if $U > c_0$. From the physical point of view this means that the current is so strong that it pulls downstream even counter-current propagating waves. As was shown, for instance, in Refs. [13–15], in a such strong current, waves on branch 3 have positive energy, whereas waves on branch 4 have negative energy.

To consider wave propagation on a spatially variable current when it accelerates or decelerates along x-axis, let us use the JWKB method, which physically presumes that the

wavelengths are much less than the characteristic scale of inhomogeneity, $\lambda \ll L$ (whereas still $\lambda \gg h$ and the shallow-water approximation is valid). This condition can be presented in the form $L/\lambda = L/(c_0 T) = L\omega/(2\pi c_0) = \hat{\omega}/2\pi \gg 1$ (where $T = 2\pi/\omega$ is the wave period) and if it is fulfilled, the JWKB solution of Eq. (8) can be sought in the form (see, e.g., [16, 17]):

$$\Phi(\xi) = \exp\left[\mathrm{i}\,\hat{\omega}\int q(\xi)\,d\xi\right], \quad q(\xi) = q_0(\xi) + \hat{\omega}^{-1}q_1(\xi) + \hat{\omega}^{-2}q_2(\xi) + \ldots \tag{12}$$

Substitution of these expressions into Eq. (8) gives two linearly independent solutions:

$$\Phi^{(\pm)}(\xi) = \sqrt{V(\xi)}\exp\left[\mathrm{i}\,\hat{\omega}\int \frac{d\xi}{V(\xi)\pm 1} + O(\hat{\omega}^{-1})\right], \tag{13}$$

and the general solution of Eq. (8) is the linear combination of these two particular solutions:

$$\Phi(x) = A_F\,\Phi^{(+)}(x) + A_B\,\Phi^{(-)}(x), \tag{14}$$

where A_F and A_B are amplitudes of co-current propagating F-wave and counter-current propagating B-wave, respectively.

In the current with a spatially varying velocity $V(\xi)$, wave propagation and transformation has a regular character, if $V(\xi) \neq 1$ (i.e., if $U(x) \neq c_0$); then Eq. (8) does not contain critical points.

In sub-critical currents, when $0 < V_{1,2} < 1$ everywhere, an incident wave arriving from the left (F-wave) or from the right (B-wave) partially transmits through the domain of inhomogeneity and partially transforms into the reflected wave of B- or F-type respectively. Notice that in this case waves of both types have positive energy.

In super-critical currents, when $V_{1,2} > 1$ is everywhere, as was mentioned above, both F-wave and B-wave can propagate only in the direction of the current; however F-wave has positive energy whereas B-wave has negative energy. An incident wave of any type propagating from left to right partially transforms into the wave of another type, so that at the infinity, $\xi \to \infty$, waves of both types appear.

In contrast to these cases, in a trans-critical current there is a critical point where $V(\xi) = 1$. The existence of such a point has only a minor influence on the co-current propagating F-wave, but exerts a crucial action on the B-wave, because its "wave number" $q_0^{(-)} \to \infty$ when $V(\xi) \to 1$. Due to this, an arbitrarily small but finite viscosity leads to dissipation of a B-wave that attains a neighborhood of the critical point. As the result of this the energy

flux J does not conserve, in general, when waves pass through this critical point. However, as will be shown below, the energy flux conserves in spatially accelerating trans-critical currents, but does not conserve in decelerating currents.

Indeed, in an accelerating current where $0 < V_1 < 1 < V_2$, an incident wave can arrive only from the left as the F-type wave only. In the sub-critical domain ($\xi < 1$) it transforms into the B-wave that runs backwards, towards $\xi = -\infty$. After passing the critical point, being in the supercritical domain ($\xi > 1$) it transforms into the B-wave that runs forward towards $\xi = +\infty$. As a result, there is no B-wave that attains the critical point; hence, there is no dissipation, and energy flux conserves. On the contrary, in decelerating currents (where $V_1 > 1 > V_2 > 0$) B-waves, no matter incident or "reflected", run to the critical point and dissipate there; therefore the energy flux does not conserve in this case.

A specific situation occurs when the incident B-wave propagates from plus infinity in the sub-critical current towards the critical point and generates an F-wave on the current inhomogeneity. If the current is super-critical on the left of the critical point, then no one wave can penetrate into that domain. Thus, the wave energy of incident B-wave partially converts into a reflected F-wave and partially absorbs in the vicinity of the critical point due to vanishingly small viscosity. We will come to the discussion of these issues in Section V when we construct exact solutions of scattering problem for Eq. (8) where it is possible.

A qualitative analysis presented above demonstrates that the most interesting results can be obtained for the trans-critical currents and that the critical points play a crucial role in such currents. However, in the vicinity of a critical point the velocity of arbitrary type $U(x)$ can be generally approximated by a linear function, $U(x) \sim x$. This makes an additional argument in favor of studying wave scattering in currents with piece-linear velocity profiles.

IV. WAVE SCATTERING IN INHOMOGENEOUS CURRENTS WITH A PIECE-LINEAR VELOCITY PROFILE

Consider now exact solutions of the problem on surface wave scattering in inhomogeneous currents with piece-linear velocity profiles described by Eqs. (9) and shown in Fig. 1. The basic equation (8) has constant coefficients out of the interval $\xi_1 < \xi < \xi_2$, where the current velocity linearly varies with ξ (either increasing or decreasing). Therefore out of this interval, solutions to this equation can be presented in terms of exponential functions with the purely

imaginary exponents describing sinusoidal travelling waves.

Within the interval $\xi_1 < \xi < \xi_2$ Eq. (8) with the help of change of variable $\zeta = \xi^2$ reduces to one of the hypergeometric equations:

$$\zeta(1-\zeta)\frac{d^2\Phi}{d\zeta^2} - (1 \mp \mathrm{i}\,\hat{\omega})\zeta\,\frac{d\Phi}{d\zeta} + \frac{\hat{\omega}^2}{4}\,\Phi = 0, \tag{15}$$

where upper sign pertains to the case of accelerating current, and lower sign – to the case of decelerating current.

The matching conditions at $\xi = \xi_1$ and $\xi = \xi_2$ are given by Eqs. (10).

A. Wave transformation in sub-critical currents

Assume first that an incident wave propagates from left to right parallel to the main current which is sub-critical in all domains, $V_1 < V_2 < 1$. As mentioned above, in the left ($\xi < \xi_1$) and right ($\xi > \xi_2$) domains Eq. (8) has constant coefficients, and in the intermediate domain ($\xi_1 < \xi < \xi_2$), where $V(\xi) = \xi$, this equation reduces to one of hypergeometric equations (15). These equations are regular in the sub-critical case, and their coefficients do not turn to zero. Two linearly independent solutions can be expressed in terms of Gauss hypergeometric function ${}_2F_1(a, b; c; \zeta)$ (see §6.4 in book [18]). Thus, the general solution of Eq. (8) for the accelerating current in three different domains can be presented as follows:

$$\Phi(\xi) = A_1 \mathrm{e}^{\mathrm{i}\kappa_1(\xi-\xi_1)} + A_2 \mathrm{e}^{-\mathrm{i}\kappa_2(\xi-\xi_1)}, \qquad \xi \le \xi_1, \tag{16}$$

$$\Phi(\xi) = B_1 w_2(\xi^2) + B_2 w_3(\xi^2), \qquad \xi_1 \le \xi \le \xi_2, \tag{17}$$

$$\Phi(\xi) = C_1 \mathrm{e}^{\mathrm{i}\kappa_3(\xi-\xi_2)} + C_2 \mathrm{e}^{-\mathrm{i}\kappa_4(\xi-\xi_2)}, \qquad \xi \ge \xi_2, \tag{18}$$

where $\kappa_1 = \hat{\omega}/(1+V_1)$, $\kappa_2 = \hat{\omega}/(1-V_1)$, $\kappa_3 = \hat{\omega}/(1+V_2)$, $\kappa_4 = \hat{\omega}/(1-V_2)$, $A_{1,2}$, $B_{1,2}$, $C_{1,2}$ are arbitrary constants, and

$$w_2(\zeta) = \zeta\,{}_2F_1(1-\mathrm{i}\,\hat{\omega}/2,\, 1-\mathrm{i}\,\hat{\omega}/2;\, 2;\zeta), \quad w_3(\zeta) = {}_2F_1(-\mathrm{i}\hat{\omega}/2, -\mathrm{i}\,\hat{\omega}/2; 1-\mathrm{i}\,\hat{\omega}; 1-\zeta). \tag{19}$$

The Wronskian of these linearly independent functions is [18]:

$$W = w_2'(\zeta)w_3(\zeta) - w_2(\zeta)w_3'(\zeta) = \frac{\Gamma(1-\mathrm{i}\,\hat{\omega})}{\Gamma^2(1-\mathrm{i}\,\hat{\omega}/2)}(1-\zeta)^{\mathrm{i}\,\hat{\omega}-1}. \tag{20}$$

Similarly the general solution of Eq. (8) for the decelerating current can be presented. In the domains $\xi < \xi_1$ and $\xi > \xi_2$ solutions are the same as above, whereas in the intermediate

domain $\xi_1 < \xi < \xi_2$ the general solution is:

$$\Phi(\xi) = B_1 \tilde{w}_2(\xi^2) + B_2 \tilde{w}_3(\xi^2), \tag{21}$$

where the linearly independent functions are

$$\tilde{w}_2(\zeta) = \zeta\, {}_2F_1(1 + \mathrm{i}\,\hat{\omega}/2,\, 1 + \mathrm{i}\,\hat{\omega}/2;\, 2; \zeta), \quad \tilde{w}_3(\zeta) = {}_2F_1(\mathrm{i}\hat{\omega}/2, \mathrm{i}\,\hat{\omega}/2; 1 + \mathrm{i}\,\hat{\omega}; 1 - \zeta). \tag{22}$$

with the Wronskian:

$$\tilde{W} = \tilde{w}_2'(\zeta)\tilde{w}_3(\zeta) - \tilde{w}_2(\zeta)\tilde{w}_3'(\zeta) = \frac{\Gamma(1 + \mathrm{i}\,\hat{\omega})}{\Gamma^2(1 + \mathrm{i}\,\hat{\omega}/2)}(1 - \zeta)^{-\mathrm{i}\,\hat{\omega}-1}. \tag{23}$$

1. Accelerating currents. Transformation of downstream propagating incident wave

Assume that the incident wave has a unit amplitude $A_1 = 1$ and calculate the transformation coefficients, setting $C_2 = 0$ and denoting the amplitudes of the reflected wave by $R \equiv A_2$ and the transmitted wave by $T \equiv C_1$ (R and T play a role of transformation coefficients, as they are usually determined in hydrodynamics – see, e.g. [19, 20] and references therein).

Using the matching conditions at the boundaries of domains (see Appendix B), we find:

$$B_1\, w_2(V_1^2) + B_2\, w_3(V_1^2) = R + 1, \tag{24}$$

$$B_1\, w_2'(V_1^2) + B_2\, w_3'(V_1^2) = \frac{\mathrm{i}\,\hat{\omega}}{2V_1}\left(\frac{1}{1 + V_1} - \frac{R}{1 - V_1}\right), \tag{25}$$

$$B_1\, w_2(V_2^2) + B_2\, w_3(V_2^2) = T, \tag{26}$$

$$B_1\, w_2'(V_2^2) + B_2\, w_3'(V_2^2) = \frac{\mathrm{i}\,\hat{\omega}}{2V_2}\frac{T}{1 + V_2}. \tag{27}$$

From these equations we derive the transformation coefficients:

$$R = \frac{1}{\Delta}\left\{\frac{\hat{\omega}^2\left[w_2(V_1^2)w_3(V_2^2) - w_2(V_2^2)w_3(V_1^2)\right]}{4V_1V_2(1+V_1)(1+V_2)} - w_2'(V_1^2)w_3'(V_2^2) + w_2'(V_2^2)w_3'(V_1^2) + \right.$$
$$\left.\frac{\mathrm{i}\,\hat{\omega}}{2}\left[\frac{w_2(V_1^2)w_3'(V_2^2) - w_2'(V_2^2)w_3(V_1^2)}{V_1(1+V_1)} - \frac{w_2(V_2^2)w_3'(V_1^2) - w_2'(V_1^2)w_3(V_2^2)}{V_2(1+V_2)}\right]\right\}, \quad (28)$$

$$T = -\frac{\mathrm{i}\,\hat{\omega}}{\Delta}\frac{(1-V_2^2)^{\mathrm{i}\hat{\omega}-1}}{V_1(1-V_1^2)}\frac{\Gamma(1-\mathrm{i}\,\hat{\omega})}{\Gamma^2(1-\mathrm{i}\,\hat{\omega}/2)}, \quad (29)$$

$$B_1 = -\frac{\mathrm{i}\,\hat{\omega}}{\Delta}\frac{1}{V_1(1-V_1^2)}\left[\frac{\mathrm{i}\,\hat{\omega}}{2V_2(1+V_2)}w_3(V_2^2) - w_3'(V_2^2)\right], \quad (30)$$

$$B_2 = \frac{\mathrm{i}\,\hat{\omega}}{\Delta}\frac{1}{V_1(1-V_1^2)}\left[\frac{\mathrm{i}\,\hat{\omega}}{2V_2(1+V_2)}w_2(V_2^2) - w_2'(V_2^2)\right], \quad (31)$$

where

$$\Delta = w_2'(V_1^2)w_3'(V_2^2) - w_2'(V_2^2)w_3'(V_1^2) + \frac{\hat{\omega}^2\left[w_2(V_1^2)w_3(V_2^2) - w_2(V_2^2)w_3(V_1^2)\right]}{4V_1V_2(1-V_1)(1+V_2)} +$$
$$\frac{\mathrm{i}\,\hat{\omega}}{2}\left[\frac{w_2(V_1^2)w_3'(V_2^2) - w_2'(V_2^2)w_3(V_1^2)}{V_1(1-V_1)} + \frac{w_2(V_2^2)w_3'(V_1^2) - w_2'(V_1^2)w_3(V_2^2)}{V_2(1+V_2)}\right]. \quad (32)$$

The modules of transformation coefficients $|T|$ and $|R|$, as well as modules of intermediate coefficients of wave excitation in the transient domain, $|B_1|$ and $|B_2|$, are shown in Fig. 4 as functions of dimensionless frequency $\hat{\omega}$ for the particular values of $V_1 = 0.1$ and $V_2 = 0.9$. Qualitatively similar graphics were obtained for other values of V_1 and V_2.

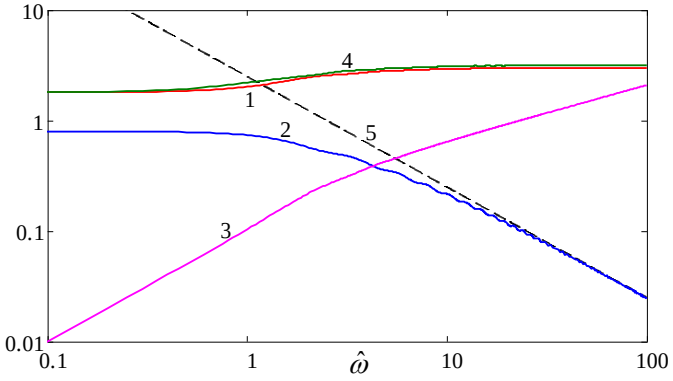


FIG. 4. (color online) Modules of transformation coefficient as functions of dimensionless frequency $\hat{\omega}$ for $V_1 = 0.1$, $V_2 = 0.9$. Line 1 – $|T|$, line 2 – $|R|$, line 3 – $|B_1|$, line 4 – $|B_2|$ Dashed line 5 represents the asymptotic for the reflection coefficient $R \sim \hat{\omega}^{-1}$.

In the long-wave approximation, when $\hat{\omega} \to 0$, the hypergeometric function ${}_2F_1(a, b; c; d)$ degenerates (see Appendix C), then the transformation coefficients reduce to

$$R = \frac{1 - V_1/V_2}{1 + V_1/V_2}, \quad T = 1 + R = \frac{2}{1 + V_1/V_2}. \tag{33}$$

These values are purely real and agree with the transformation coefficients derived in Ref. [15] for surface waves in a duct with the stepwise change of cross-section and velocity profile, and such an agreement takes place also for other wave-current configurations considered below. Notice only that here the transformation coefficients are presented in terms of velocity potential φ, whereas in Ref. [15] they are presented in terms of free surface elevation η. The relationship between these quantities is given in the end of Appendix A).

In Fig. 5a) we present the graphic of $|\Phi(\xi)|$ (see line 1) as per Eqs. (16)–(18) with $A_1 = 1$ and other determined transformation coefficients $A_2 = R$ as per Eq. (28), $C_1 = T$ as per Eq. (29), and $C_2 = 0$. Coefficients B_1 and B_2 are given by Eqs. (30) and (31). The plot was generated for the particular value of $\hat{\omega} = 1$; for other values of $\hat{\omega}$ the graphics are qualitatively similar.

The solution obtained should be in consistency with the energy flux conservation [14, 15], which is derived in Appendix A in terms of the velocity potential φ:

$$V_2 \left(1 - |R|^2\right) = V_1 |T|^2. \tag{34}$$

Substituting here the transformation coefficients R and T from Eqs. (28) and (29), we confirm that Eq. (34) reduces to the identity.

To characterize the rate of energy flux transmission, one can introduce the energy transmission factor

$$K_T = \frac{V_1}{V_2} |T|^2 \quad \overset{\hat{\omega} \to 0}{\longrightarrow} \quad \frac{4V_1/V_2}{\left(1 + V_1/V_2\right)^2}. \tag{35}$$

Then one can see that although the modulus of the transmission coefficient is greater than one (see line 1 in Fig. 4) the total energy flux (34) through the duct cross-section conserves because the cross-section decreases in the transition from the left to right domain, and the transmitted energy flux is less than the incident one ($K_T < 1$).

2. Accelerating currents. Transformation of upstream propagating incident wave

If the incident wave arrives from plus infinity, then we set in Eqs. (16) and (18) its amplitude $C_2 = 1$, the amplitude of reflected wave $C_1 = R$, and the amplitude of transmitted

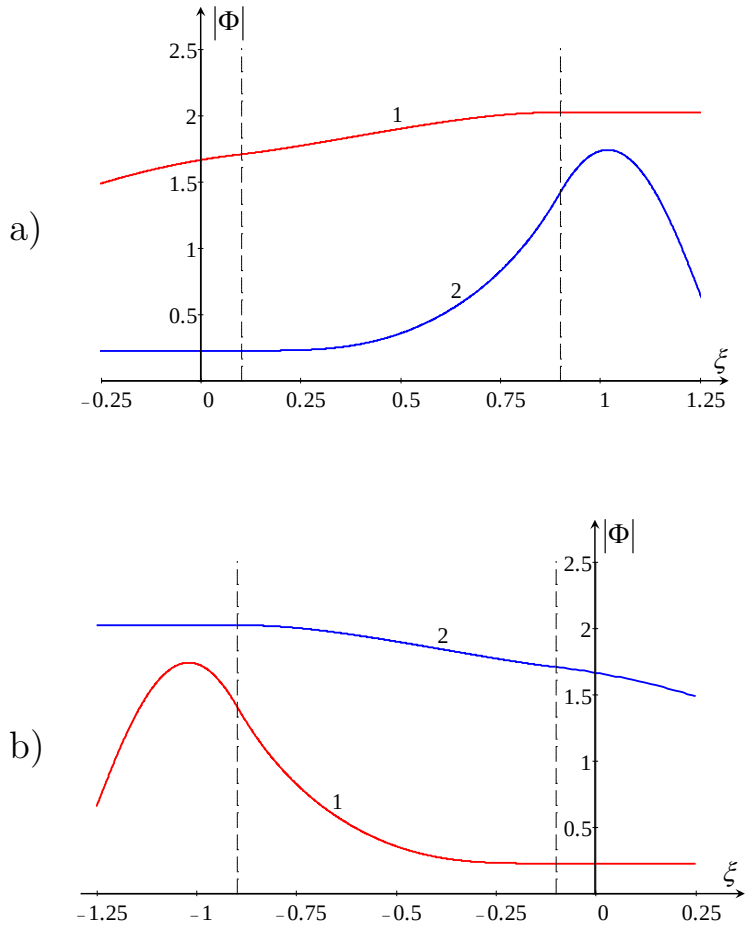


FIG. 5. (color online) Modules of function $\Phi(\xi)$ for wave scattering in accelerating (a) and decelerating (b) sub-critical currents with $V_1 = 0.1$ and $V_2 = 0.9$ in the former case and $V_1 = 0.9$ and $V_2 = 0.1$ in the latter case. Line 1 in each frame pertains to the co-current propagating incident wave, and line 2 – to the counter-current propagating incident wave. Dashed vertical lines show the boundaries of the transient domain ξ_1 and ξ_2 where the speed of the background current linearly changes.

wave $A_2 = T$, whereas $A_1 = 0$. Then from the matching conditions we obtain

$$B_1\, w_2(V_1^2) + B_2\, w_3(V_1^2) = T, \tag{36}$$

$$B_1\, w_2'(V_1^2) + B_2\, w_3'(V_1^2) = -\frac{\mathrm{i}\,\hat{\omega}}{2V_1}\frac{T}{1-V_1}, \tag{37}$$

$$B_1\, w_2(V_2^2) + B_2\, w_3(V_2^2) = 1 + R, \tag{38}$$

$$B_1\, w_2'(V_2^2) + B_2\, w_3'(V_2^2) = -\frac{\mathrm{i}\,\hat{\omega}}{2V_2}\left(\frac{1}{1-V_2} - \frac{R}{1+V_2}\right). \tag{39}$$

Solution of this set of equations is:

$$R = \frac{1}{\Delta}\left\{\frac{\hat{\omega}^2\left[w_2(V_1^2)w_3(V_2^2) - w_2(V_2^2)w_3(V_1^2)\right]}{4V_1V_2(1-V_1)(1-V_2)} - w_2'(V_1^2)w_3'(V_2^2) + w_2'(V_2^2)w_3'(V_1^2) - \right.$$
$$\left.\frac{\mathrm{i}\,\hat{\omega}}{2}\left[\frac{w_2(V_1^2)w_3'(V_2^2) - w_2'(V_2^2)w_3(V_1^2)}{V_1(1-V_1)} - \frac{w_2(V_2^2)w_3'(V_1^2) - w_2'(V_1^2)w_3(V_2^2)}{V_2(1-V_2)}\right]\right\}, \quad (40)$$

$$T = -\frac{\mathrm{i}\,\hat{\omega}}{\Delta}\frac{(1-V_1^2)^{\mathrm{i}\,\hat{\omega}-1}}{V_2(1-V_2^2)}\,\frac{\Gamma(1-\mathrm{i}\,\hat{\omega})}{\Gamma^2(1-\mathrm{i}\,\hat{\omega}/2)}\,, \quad (41)$$

$$B_1 = \frac{\mathrm{i}\,\hat{\omega}}{\Delta}\frac{1}{V_2(1-V_2^2)}\left[\frac{\mathrm{i}\,\hat{\omega}}{2V_1(1-V_1)}\,w_3(V_1^2) + w_3'(V_1^2)\right], \quad (42)$$

$$B_2 = -\frac{\mathrm{i}\,\hat{\omega}}{\Delta}\frac{1}{V_2(1-V_2^2)}\left[\frac{\mathrm{i}\,\hat{\omega}}{2V_1(1-V_1)}\,w_2(V_1^2) + w_2'(V_1^2)\right], \quad (43)$$

where Δ is the same as in Eq. (32).

In the long-wave approximation, $\hat{\omega} \to 0$, we obtain the limiting values of transformation coefficients

$$R = \frac{1 - V_2/V_1}{1 + V_2/V_1}, \quad T = 1 + R = \frac{2}{1 + V_2/V_1}. \quad (44)$$

These values again are purely real and agree with the transformation coefficients derived in Ref. [15] for surface waves in a duct with the stepwise change of cross-section and velocity profile.

This solution is also in consistency with the energy flux conservation, which now takes the form:

$$V_1\left(1 - |R|^2\right) = V_2|T|^2. \quad (45)$$

Substituting here the expressions for the transformation coefficients, (40) and (41), we confirm that Eq. (45) reduces to the identity. The energy transmission factor K_T in the limit $\hat{\omega} \to 0$ remains the same as in Eq. (35).

The graphic of $|\Phi(\xi)|$ is presented in Fig. 5a) by line 2. The plot was generated on the basis of solution (16)–(18) with $C_2 = 1$, $A_1 = 0$ and other determined transformation coefficients $C_1 = R$ as per Eq. (40) and $A_2 = T$ as per Eq. (41). Coefficients B_1 and B_2 are given by Eqs. (42) and (43).

3. Wave transformation in a decelerating sub-critical current

The decelerating current can occur, for example, in a widening duct. To calculate the transformation coefficients of waves in a decelerating current with a piece-linear profile it is convenient to choose the origin of coordinate frame such as shown in Fig. 1b).

The general solutions of the basic equation (8) in the left and right domains beyond the interval $\xi_1 < \xi < \xi_2$ are the same as in Eqs. (16) and (18), whereas in the transient domain the solution is given by Eq. (21).

To calculate the transformation coefficients one can repeat the simple, but tedious calculations similar to the presented above. The result shows that the expressions for the transformation coefficients remain the same as in Eqs. (28)–(32) for the co-current propagating incident wave and Eqs. (40)–(43), and (32) for the counter-current propagating incident wave, but in both these cases $\hat{\omega}$ should be replaced by $-\hat{\omega}$ and w_i by $\tilde{w}_i$. The energy flux Eq. (34) for the co-current propagating incident wave or Eq. (45) for the counter-current propagating incident wave conserves in these cases too.

The graphics of $|\Phi(\xi)|$ are presented in Fig. 5b) by line 1 for co-current propagating incident wave, and by line 2 for counter-current propagating incident wave.

B. Wave transformation in a super-critical current

Assume now that the main current is super-critical everywhere, $V_2 > V_1 > 1$. In this case, there are no upstream propagating waves. Indeed in such strong current even waves propagating with the speed $-c_0$ in the frame moving with the water are pulled downstream by the current whose speed $U > c_0$, therefore in the immovable laboratory frame the speed of such "counter-current" propagating waves is $U - c_0 > 0$. Such waves possess a negative energy (see, for instance, [13–15]). Thus, the problem statement can contain an incident sinusoidal wave propagating only downstream from the $\xi < \xi_1$ domain; the wave can be of either positive energy with $\hat{\omega} = (V_1 + 1)\kappa_1$ or negative energy with $\hat{\omega} = (V_1 - 1)\kappa_2$. After transformation on the inhomogeneous current in the interval $\xi_1 < \xi < \xi_2$ these waves produce two transmitted waves in the right domain, $\xi > \xi_2$ one of positive energy and another of negative energy. Below we consider such transformation in detail.

In the super-critical case the basic equation (8) is also regular and its coefficients do

not turn to zero. To construct its solutions in the intermediate domain $\xi_1 \le \xi \le \xi_2$ it is convenient to re-write the equation in slightly different form:

$$\eta(1-\eta)\frac{d^2\Psi}{d\eta^2} + [1-(2\mp \mathrm{i}\,\hat{\omega})\eta]\,\frac{d\Psi}{d\eta} \pm \frac{\mathrm{i}\,\hat{\omega}}{2}\left(1\mp\frac{\mathrm{i}\,\hat{\omega}}{2}\right)\Psi = 0, \tag{46}$$

where $\eta = 1/\zeta$, $\Psi(\eta) = \eta^{\pm \mathrm{i}\hat{\omega}/2}\Phi$, upper signs pertain to the accelerating current, and lower signs – to the decelerating currents.

Solutions of Eq. (8) in the domains where the current speed is constant are

$$\Phi(\xi) = A_1 \mathrm{e}^{\mathrm{i}\kappa_1(\xi-\xi_1)} + A_2 \mathrm{e}^{\mathrm{i}\kappa_2(\xi-\xi_1)}, \qquad \xi \le \xi_1, \tag{47}$$

$$\Phi(\xi) = C_1 \mathrm{e}^{\mathrm{i}\kappa_3(\xi-\xi_2)} + C_2 \mathrm{e}^{\mathrm{i}\kappa_4(\xi-\xi_2)}, \qquad \xi \ge \xi_2, \tag{48}$$

were $\kappa_1 = \hat{\omega}/(V_1+1)$, $\kappa_2 = \hat{\omega}/(V_1-1)$, $\kappa_3 = \hat{\omega}/(V_2+1)$, $\kappa_4 = \hat{\omega}/(V_2-1)$.

In the intermediate domain $\xi_1 \le \xi \le \xi_2$ the solution of hypergeometric Eq. (46) in the case of accelerating current is

$$\Phi(\xi) = \xi^{\mathrm{i}\hat{\omega}}\left[B_1 \breve{w}_1\left(\xi^{-2}\right) + B_2 \breve{w}_3\left(\xi^{-2}\right)\right], \tag{49}$$

where two linearly independent solutions of Eq. (46) can be chosen in the form (see §6.4 in the book [18]):

$$\breve{w}_1(\eta) = {}_2F_1(-\mathrm{i}\,\hat{\omega}/2,\, 1-\mathrm{i}\,\hat{\omega}/2;\, 1;\eta), \quad \breve{w}_3(\eta) = {}_2F_1(-\mathrm{i}\hat{\omega}/2, 1-\mathrm{i}\,\hat{\omega}/2; 1-\mathrm{i}\,\hat{\omega}; 1-\eta) \tag{50}$$

with the Wronskian

$$\breve{W} = \breve{w}_1'(\eta)\breve{w}_3(\eta) - \breve{w}_1(\eta)\breve{w}_3'(\eta) = \frac{(1-\eta)^{\mathrm{i}\,\hat{\omega}-1}}{\eta}\frac{\Gamma(1-\mathrm{i}\,\hat{\omega})}{\Gamma(-\mathrm{i}\,\hat{\omega}/2)\Gamma(1-\mathrm{i}\,\hat{\omega}/2)}. \tag{51}$$

In the case of decelerating current the solution of hypergeometric Eq. (46) is

$$\Phi(\xi) = (-\xi)^{-\mathrm{i}\,\hat{\omega}}\left[B_1 \hat{w}_1\left(\xi^{-2}\right) + B_2 \hat{w}_3\left(\xi^{-2}\right)\right], \tag{52}$$

and linearly independent solutions can be chosen in the form:

$$\hat{w}_1(\eta) = {}_2F_1(\mathrm{i}\,\hat{\omega}/2,\, 1+\mathrm{i}\,\hat{\omega}/2;\, 1;\eta), \quad \hat{w}_3(\eta) = {}_2F_1(\mathrm{i}\hat{\omega}/2, 1+\mathrm{i}\,\hat{\omega}/2; 1+\mathrm{i}\,\hat{\omega}; 1-\eta) \tag{53}$$

with the Wronskian

$$\hat{W} = \hat{w}_1'(\eta)\hat{w}_3(\eta) - \hat{w}_1(\eta)\hat{w}_3'(\eta) = \frac{(1-\eta)^{-\mathrm{i}\,\hat{\omega}-1}}{\eta}\frac{\Gamma(1+\mathrm{i}\,\hat{\omega})}{\Gamma(\mathrm{i}\,\hat{\omega}/2)\Gamma(1+\mathrm{i}\,\hat{\omega}/2)}. \tag{54}$$

1. Transformation of a positive-energy wave in an accelerating current

Consider first transformation of a positive energy incident wave (see line 3 in Fig. 3) with the unit amplitude ($A_1 = 1$, $A_2 = 0$). Matching the solutions in different current domains and using the chain rule $d/d\xi = -2\xi^{-3}d/d\eta$, we obtain at $\xi = \xi_1$:

$$B_1\,\breve{w}_1(V_1^{-2}) + B_2\,\breve{w}_3(V_1^{-2}) = V_1^{-\mathrm{i}\hat{\omega}}, \tag{55}$$

$$B_1\,\breve{w}_1'(V_1^{-2}) + B_2\,\breve{w}_3'(V_1^{-2}) = \frac{\mathrm{i}\,\hat{\omega}}{2}\frac{V_1^{2-\mathrm{i}\hat{\omega}}}{V_1+1}, \tag{56}$$

where prime stands for a derivative of a corresponding function with respect to its entire argument.

Similarly from the matching conditions at $\xi = \xi_2$ we obtain:

$$C_1 + C_2 = V_2^{\mathrm{i}\hat{\omega}}\left[B_1\,\breve{w}_1(V_2^{-2}) + B_2\,\breve{w}_3(V_2^{-2})\right], \tag{57}$$

$$(V_2-1)C_1 - (V_2+1)C_2 = -\frac{2\mathrm{i}}{\hat{\omega}}\,V_2^{\mathrm{i}\hat{\omega}-2}(V_2^2-1)\left[B_1\,\breve{w}_1'(V_2^{-2}) + B_2\,\breve{w}_3'(V_2^{-2})\right]. \tag{58}$$

From Eqs. (55) and (56) we find

$$B_1 = -\frac{\Gamma(-\mathrm{i}\,\hat{\omega}/2)\,\Gamma(1-\mathrm{i}\,\hat{\omega}/2)}{\Gamma(1-\mathrm{i}\,\hat{\omega})}\,V_1^{\mathrm{i}\hat{\omega}-2}\left(V_1^2-1\right)^{1-\mathrm{i}\hat{\omega}}\left[\frac{\breve{w}_3'(V_1^{-2})}{V_1^2} - \frac{\mathrm{i}\,\hat{\omega}\,\breve{w}_3(V_1^{-2})}{2(V_1+1)}\right], \tag{59}$$

$$B_2 = \frac{\Gamma(-\mathrm{i}\,\hat{\omega}/2)\,\Gamma(1-\mathrm{i}\,\hat{\omega}/2)}{\Gamma(1-\mathrm{i}\,\hat{\omega})}\,V_1^{\mathrm{i}\hat{\omega}-2}\left(V_1^2-1\right)^{1-\mathrm{i}\hat{\omega}}\left[\frac{\breve{w}_1'(V_1^{-2})}{V_1^2} - \frac{\mathrm{i}\,\hat{\omega}\,\breve{w}_1(V_1^{-2})}{2(V_1+1)}\right]. \tag{60}$$

Substituting these in Eqs. (57) and (58), we find the transmission coefficients for the positive energy mode $T_p \equiv C_1$ and negative energy mode $T_n \equiv C_2$:

$$T_p = -\frac{\Gamma^2(-\mathrm{i}\,\hat{\omega}/2)}{2\Gamma(1-\mathrm{i}\,\hat{\omega})}\,V_1^{\mathrm{i}\hat{\omega}-2}V_2^{\mathrm{i}\hat{\omega}-1}\left(V_1^2-1\right)^{1-\mathrm{i}\hat{\omega}}\left(V_2^2-1\right)\times$$

$$\left\{\frac{\breve{w}_1'(V_1^{-2})\breve{w}_3'(V_2^{-2}) - \breve{w}_1'(V_2^{-2})\breve{w}_3'(V_1^{-2})}{V_1^2V_2^2} + \frac{\hat{\omega}^2}{4}\,\frac{\breve{w}_1(V_1^{-2})\breve{w}_3(V_2^{-2}) - \breve{w}_1(V_2^{-2})\breve{w}_3(V_1^{-2})}{(V_1+1)(V_2-1)} + \right.$$

$$\left.\frac{\mathrm{i}\,\hat{\omega}}{2}\left[\frac{\breve{w}_1'(V_1^{-2})\breve{w}_3(V_2^{-2}) - \breve{w}_1(V_2^{-2})\breve{w}_3'(V_1^{-2})}{V_1^2(V_2-1)} - \frac{\breve{w}_1(V_1^{-2})\breve{w}_3'(V_2^{-2}) - \breve{w}_1'(V_2^{-2})\breve{w}_3(V_1^{-2})}{V_2^2(V_1+1)}\right]\right\}, \tag{61}$$

$$T_n = \frac{\Gamma^2(-\mathrm{i}\,\hat{\omega}/2)}{2\Gamma(1-\mathrm{i}\,\hat{\omega})}\,V_1^{\mathrm{i}\hat{\omega}-2}V_2^{\mathrm{i}\hat{\omega}-1}\left(V_1^2-1\right)^{1-\mathrm{i}\hat{\omega}}\left(V_2^2-1\right)\times$$

$$\left\{\frac{\breve{w}_1'(V_1^{-2})\breve{w}_3'(V_2^{-2})-\breve{w}_1'(V_2^{-2})\breve{w}_3'(V_1^{-2})}{V_1^2V_2^2}-\frac{\hat{\omega}^2}{4}\,\frac{\breve{w}_1(V_1^{-2})\breve{w}_3(V_2^{-2})-\breve{w}_1(V_2^{-2})\breve{w}_3(V_1^{-2})}{(V_1+1)(V_2+1)}-\right.$$
$$\left.\frac{\mathrm{i}\,\hat{\omega}}{2}\left[\frac{\breve{w}_1'(V_1^{-2})\breve{w}_3(V_2^{-2})-\breve{w}_1(V_2^{-2})\breve{w}_3'(V_1^{-2})}{V_1^2(V_2+1)}+\frac{\breve{w}_1(V_1^{-2})\breve{w}_3'(V_2^{-2})-\breve{w}_1'(V_2^{-2})\breve{w}_3(V_1^{-2})}{V_2^2(V_1+1)}\right]\right\}. \quad (62)$$

The modules of transformation coefficients $|T_p|$ and $|T_n|$ together with the intermediate coefficients of wave excitation in the transient zone $|B_1|$ and $|B_2|$ are shown below in Fig. 6a) as functions of dimensionless frequency $\hat{\omega}$ for the particular values of $V_1 = 1.1$ and $V_2 = 1.9$. Qualitatively similar graphics were obtained for other values of V_1 and V_2.

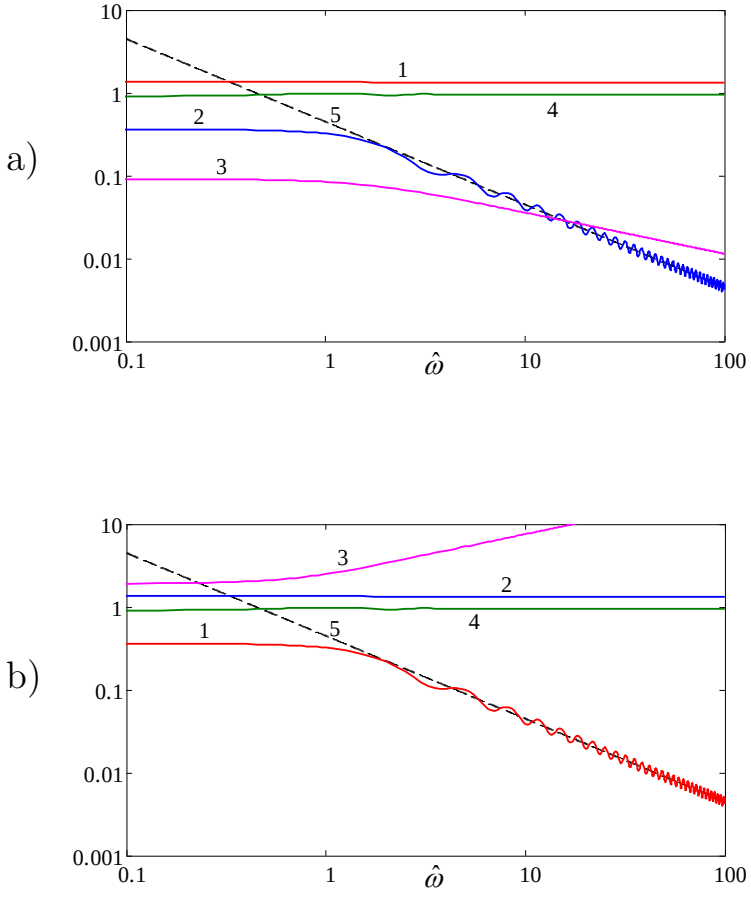


FIG. 6. (color online) Modules of transformation coefficient as functions of dimensionless frequency $\hat{\omega}$ when a positive energy wave scatters (panel a) and negative energy wave scatters (panel b) in the current with $V_1 = 1.1$, $V_2 = 1.9$. Line 1 – $|T_p|$, line 2 – $|T_n|$, line 3 – $|B_1|$, line 4 – $|B_2|$. Dashed lines 5 represent the asymptotics for $|T_n| \sim \hat{\omega}^{-1}$ in panel a) and for $|T_p| \sim \hat{\omega}^{-1}$ in panel b).

In Fig. 7a) we present graphics of $|\Phi(\xi)|$ as per Eqs. (47)–(49) for $A_1 = 1$, $A_2 = 0$, $C_1 = T_p$ as per Eq. (61), and $C_2 = T_n$ as per Eq. (62). Coefficients B_1 and B_2 are given by Eqs. (59)

and (60). The plot was generated for two particular values of frequency, $\hat{\omega} = 1$ (line 1), and $\hat{\omega} = 100$ (line 2).

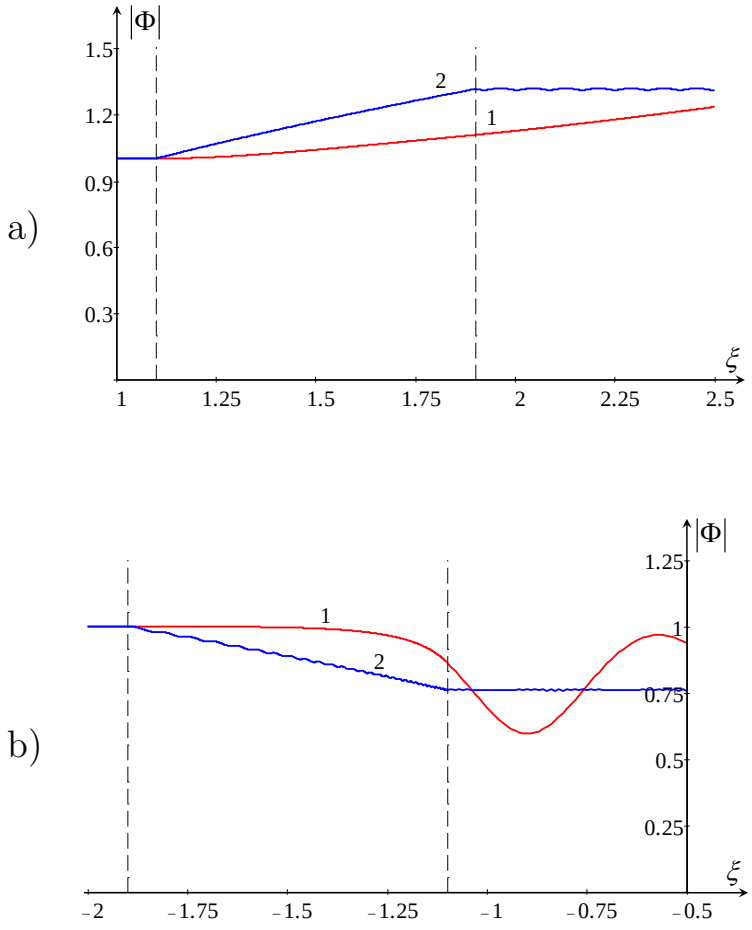


FIG. 7. (color online) Module of function $\Phi(\xi)$ for the scattering of positive- and negative-energy waves in accelerating with $V_1 = 1.1$ and $V_2 = 1.9$ (frame a) and decelerating with $V_1 = 1.9$ and $V_2 = 1.1$ (frame b) super-critical currents for two particular values of frequency, $\hat{\omega} = 1$ (line 1), and $\hat{\omega} = 100$ (line 2).

The transmission coefficients are in consistency with the energy flux conservation law which has the following form:

$$J = \frac{2\hat{\omega}}{V_1} = \frac{2\hat{\omega}}{V_2}\left(|T_p|^2 - |T_n|^2\right) \quad \text{or} \quad |T_p|^2 - |T_n|^2 = \frac{V_2}{V_1}. \tag{63}$$

If we introduce two energy transmission factors, for positive- and negative-energy waves,

$$K_{Tp} = \frac{V_1}{V_2}|T_p|^2 \quad \text{and} \quad K_{Tn} = \frac{V_1}{V_2}|T_n|^2, \tag{64}$$

then we can see that both waves grow in such a manner that $K_{Tp} - K_{Tn} = 1$. This means that the positive-energy wave not only dominates in the right domain (cf. lines 1 and 2 in Fig. 6a), but it also carries a greater energy flux than the incident one. Moreover, with a proper choice of V_1 and V_2 even the energy flux of negative-energy wave can become greater by modulus than that of incident wave, $K_{Tn} > 1$. Then we have $K_{Tp} > K_{Tn} > 1$. Figure 8 illustrates the dependences of energy transmission factors on the frequency for relatively small increase of current speed ($V_1 = 1.1$, $V_2 = 1.9$) and big increase of current speed ($V_1 = 1.1$, $V_2 = 8.0$). In the latter case both K_{Tp} and K_{Tn} are greater than 1 in a certain range of frequencies $\hat{\omega} < \hat{\omega}_c$.

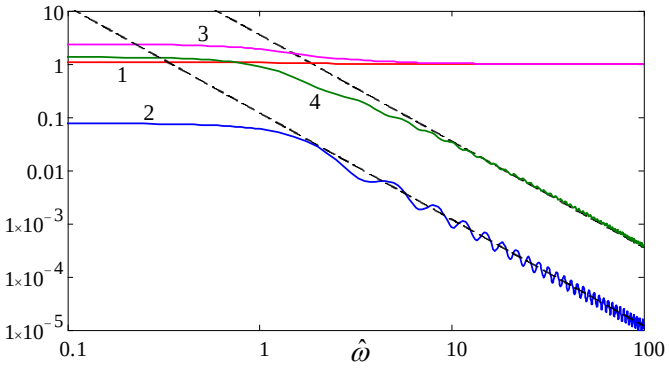


FIG. 8. (color online) The dependences of energy transmission factors K_{Tp} and K_{Tn} on the frequency for a relatively small increase of current speed ($V_1 = 1.1$, $V_2 = 1.9$), lines 1 and 2 respectively, and a large increase of current speed ($V_1 = 1.1$, $V_2 = 8.0$), lines 3 and 4 respectively. Inclined dashed lines show the asymptotic dependences $K_{Tn} \sim \hat{\omega}^{-2}$.

In the long-wave approximation, $\hat{\omega} \to 0$ (see Appendix C) we obtain (cf. [15]):

$$T_p = \frac{1 + V_1/V_2}{2V_1/V_2}, \quad T_n = -\frac{1 - V_1/V_2}{2V_1/V_2}, \quad K_{Tp} = \frac{(1 + V_1/V_2)^2}{4V_1/V_2}, \quad K_{Tn} = \frac{(1 - V_1/V_2)^2}{4V_1/V_2}. \quad (65)$$

2. Transformation of negative-energy wave in an accelerating current

Consider now transformation of a negative energy incident wave (see line 4 in Fig. 3) with unit amplitude ($A_1 = 0$, $A_2 = 1$). From the matching conditions at $\xi = \xi_1$ we obtain:

$$B_1\, \breve{w}_1(V_1^{-2}) + B_2\, \breve{w}_3(V_1^{-2}) = V_1^{-\mathrm{i}\hat{\omega}}, \quad (66)$$

$$B_1\, \breve{w}_1'(V_1^{-2}) + B_2\, \breve{w}_3'(V_1^{-2}) = -\frac{\mathrm{i}\,\hat{\omega}}{2}\frac{V_1^{2-\mathrm{i}\hat{\omega}}}{V_1 - 1}. \quad (67)$$

The matching conditions at $\xi = \xi_2$ remain the same as in Eqs. (57) and (58).

From Eqs. (66) and (67) we find

$$B_1 = -\frac{\Gamma(-\mathrm{i}\,\hat{\omega}/2)\,\Gamma(1-\mathrm{i}\,\hat{\omega}/2)}{\Gamma(1-\mathrm{i}\,\hat{\omega})}\,V_1^{\mathrm{i}\hat{\omega}-2}\left(V_1^2-1\right)^{1-\mathrm{i}\hat{\omega}}\left[\frac{\breve{w}_3'(V_1^{-2})}{V_1^2}+\frac{\mathrm{i}\,\hat{\omega}\,\breve{w}_3(V_1^{-2})}{2(V_1-1)}\right], \quad (68)$$

$$B_2 = \frac{\Gamma(-\mathrm{i}\,\hat{\omega}/2)\,\Gamma(1-\mathrm{i}\,\hat{\omega}/2)}{\Gamma(1-\mathrm{i}\,\hat{\omega})}\,V_1^{\mathrm{i}\hat{\omega}-2}\left(V_1^2-1\right)^{1-\mathrm{i}\hat{\omega}}\left[\frac{\breve{w}_1'(V_1^{-2})}{V_1^2}+\frac{\mathrm{i}\,\hat{\omega}\,\breve{w}_1(V_1^{-2})}{2(V_1-1)}\right]. \quad (69)$$

Substituting these in Eqs. (57) and (58), we find the transmission coefficients for the positive energy mode $T_p \equiv C_1$ and negative energy mode $T_n \equiv C_2$:

$$T_p = -\frac{\Gamma^2(-\mathrm{i}\,\hat{\omega}/2)}{2\Gamma(1-\mathrm{i}\,\hat{\omega})}\,V_1^{\mathrm{i}\hat{\omega}-2}V_2^{\mathrm{i}\hat{\omega}-1}\left(V_1^2-1\right)^{1-\mathrm{i}\hat{\omega}}\left(V_2^2-1\right)\times$$
$$\left\{\frac{\breve{w}_1'(V_1^{-2})\breve{w}_3'(V_2^{-2})-\breve{w}_1'(V_2^{-2})\breve{w}_3'(V_1^{-2})}{V_1^2V_2^2}-\frac{\hat{\omega}^2}{4}\,\frac{\breve{w}_1(V_1^{-2})\breve{w}_3(V_2^{-2})-\breve{w}_1(V_2^{-2})\breve{w}_3(V_1^{-2})}{(V_1-1)(V_2-1)}+\right.$$
$$\left.\frac{\mathrm{i}\,\hat{\omega}}{2}\left[\frac{\breve{w}_1'(V_1^{-2})\breve{w}_3(V_2^{-2})-\breve{w}_1(V_2^{-2})\breve{w}_3'(V_1^{-2})}{V_1^2(V_2-1)}+\frac{\breve{w}_1(V_1^{-2})\breve{w}_3'(V_2^{-2})-\breve{w}_1'(V_2^{-2})\breve{w}_3(V_1^{-2})}{V_2^2(V_1-1)}\right]\right\}, \quad (70)$$

$$T_n = \frac{\Gamma^2(-\mathrm{i}\,\hat{\omega}/2)}{2\Gamma(1-\mathrm{i}\,\hat{\omega})}\,V_1^{\mathrm{i}\hat{\omega}-2}V_2^{\mathrm{i}\hat{\omega}-1}\left(V_1^2-1\right)^{1-\mathrm{i}\hat{\omega}}\left(V_2^2-1\right)\times$$
$$\left\{\frac{\breve{w}_1'(V_1^{-2})\breve{w}_3'(V_2^{-2})-\breve{w}_1'(V_2^{-2})\breve{w}_3'(V_1^{-2})}{V_1^2V_2^2}+\frac{\hat{\omega}^2}{4}\,\frac{\breve{w}_1(V_1^{-2})\breve{w}_3(V_2^{-2})-\breve{w}_1(V_2^{-2})\breve{w}_3(V_1^{-2})}{(V_1-1)(V_2+1)}-\right.$$
$$\left.\frac{\mathrm{i}\,\hat{\omega}}{2}\left[\frac{\breve{w}_1'(V_1^{-2})\breve{w}_3(V_2^{-2})-\breve{w}_1(V_2^{-2})\breve{w}_3'(V_1^{-2})}{V_1^2(V_2+1)}-\frac{\breve{w}_1(V_1^{-2})\breve{w}_3'(V_2^{-2})-\breve{w}_1'(V_2^{-2})\breve{w}_3(V_1^{-2})}{V_2^2(V_1-1)}\right]\right\}. \quad (71)$$

The modules of transformation coefficients $|T_p|$ and $|T_n|$ together with the intermediate coefficients of wave excitation in the transient zone $|B_1|$ and $|B_2|$ are shown in Fig. 6b) as functions of dimensionless frequency $\hat{\omega}$ for the particular values of $V_1 = 1.1$ and $V_2 = 1.9$. Qualitatively similar graphics were obtained for other values of V_1 and V_2. The graphic of $|\Phi(\xi)|$ is the same as the graphic shown in Fig. 7a) for the case of scattering of positive-energy incident wave.

The transmission coefficients are again in consistency with the energy flux conservation law which now has the following form:

$$J = -\frac{2\hat{\omega}}{V_1} = -\frac{2\hat{\omega}}{V_2}\left(|T_n|^2-|T_p|^2\right) \quad \text{or} \quad |T_n|^2-|T_p|^2 = \frac{V_2}{V_1}. \quad (72)$$

As follows from this equation, the energy flux J is negative everywhere, and the negative energy wave dominates in the right domain (cf. lines 1 and 2 in Fig. 6b). Both transmitted

waves grow in a such manner that the energy transmission factors (see Eq. (64)) obey the equality $K_{Tn} - K_{Tp} = 1$. Thus, the negative-energy wave not only dominates in the right domain, but also carries a greater energy flux than the incident wave. At a certain relationship between V_1 and V_2 the energy fluxes of positive- and negative-energy waves can be greater on absolute value than that of incident wave, then we have $K_{Tn} > K_{Tp} > 1$.

In the long-wave approximation, $\hat{\omega} \to 0$, we obtain (see Appendix C):

$$T_p = -\frac{1 - V_1/V_2}{2V_1/V_2}, \quad T_n = \frac{1 + V_1/V_2}{2V_1/V_2}, \quad K_{Tp} = \frac{(1 - V_1/V_2)^2}{4V_1/V_2}, \quad K_{Tn} = \frac{(1 + V_1/V_2)^2}{4V_1/V_2}, \quad (73)$$

i.e., in comparison with Eqs. (65), the energy transmission factors are interchanged. The values of transmission coefficients are purely real, but now $T_p < 0$ and $T_n > 0$; they are in agreement with results derived in Ref. [15].

3. Wave transformation in a decelerating super-critical current

In the case of decelerating super-critical current ($V_1 > V_2 > 1$) the configuration of the incident wave and current is the same as above in this subsection. Again there is no reflected wave in the left domain $\xi < \xi_1$ and there are two transmitted waves in the right domain $\xi > \xi_2$.

The main equation describing wave propagation is the same as Eq. (46) with only formal replacement of $\hat{\omega}$ by $-\hat{\omega}$. The general solutions of the basic equation (8) in the left and right domains beyond the interval $\xi_1 < \xi < \xi_2$ are the same as in Eqs. (47) and (48), whereas in the transient domain the solution is given by Eq. (52).

To calculate the transformation coefficients one can repeat the simple, but tedious calculations similar to those presented above. The result shows that the expressions for the transformation coefficients remain the same as in Eqs. (61) and (62) for the incident wave of positive energy and Eqs. (70) and (71) for the incident wave of negative energy, but in both these cases $\hat{\omega}$ should be replaced by $-\hat{\omega}$ and $\breve{w}_i$ by $\hat{w}_i$. The corresponding energy fluxes for the incident waves of positive and negative energies conserve, and Eqs. (63) and Eq. (72) remain the same in these cases too.

The graphics of $|\Phi(\xi)|$ for the scattering of positive- and negative-energy waves are also the same in the decelerating currents. They are shown in Fig. 7b) in the subsubsection IV B 1 for two particular values of frequency, $\hat{\omega} = 1$ (line 1), and $\hat{\omega} = 100$ (line 2).

C. Wave transformation in trans-critical accelerating currents $0 < V_1 < 1 < V_2$

The specific feature of a trans-critical current is the transition of the background current speed $U(x)$ through the critical wave speed c_0. In this case the basic equation (8) contains a singular point where $V = 1$, therefore the behavior of solutions in the vicinity of this point should be thoroughly investigated.

The general solution of Eq. (8) in different intervals of ξ-axis can be presented in the form:

$$\Phi(\xi) = A_1 e^{\mathrm{i}\,\kappa_1(\xi-\xi_1)} + A_2 e^{-\mathrm{i}\,\kappa_2(\xi-\xi_1)}, \quad \xi < \xi_1, \tag{74}$$

$$\Phi(\xi) = B_1 w_2(\xi^2) + B_2 w_3(\xi^2), \qquad \xi_1 < \xi < 1, \tag{75}$$

$$\Phi(\xi) = \xi^{\mathrm{i}\,\hat\omega}\left[\breve B_1\,\breve w_1(\xi^{-2}) + \breve B_2\,\breve w_3(\xi^{-2})\right],\ 1 < \xi < \xi_2, \tag{76}$$

$$\Phi(\xi) = C_1\, e^{\mathrm{i}\,\kappa_3(\xi-\xi_2)} + C_2\, e^{-\mathrm{i}\,\kappa_4(\xi-\xi_2)}, \quad \xi > \xi_2, \tag{77}$$

where $\kappa_1 = \hat\omega/(1+V_1)$, $\kappa_2 = \hat\omega/(1-V_1)$, $\kappa_3 = \hat\omega/(V_2+1)$, and $\kappa_4 = \hat\omega/(V_2-1)$.

To pass through the singular point where $V(\xi) = 1$, let us consider asymptotic behavior of solution $\Phi(\xi)$ in the vicinity of the point $\xi = 1$. To this end we use the formula valid for $|\arg(1-x)| < \pi$ (see [21], formula 9.131.2.):

$$\begin{aligned} {}_2F_1(a,b;c;x) = {} & \frac{\Gamma(c)\,\Gamma(c-a-b)}{\Gamma(c-a)\,\Gamma(c-b)}\,{}_2F_1(a,b;a+b-c+1;1-x) + \\ & \frac{\Gamma(c)\,\Gamma(a+b-c)}{\Gamma(a)\,\Gamma(b)}\,(1-x)^{c-a-b}\,{}_2F_1(c-a,c-b;c-a-b+1;1-x). \end{aligned} \tag{78}$$

With the help of this formula let us present the asymptotic expansion of functions (75) and (76), keeping only the leading terms:

$$\Phi(\xi) = B_2 + \frac{\Gamma(\mathrm{i}\,\hat\omega)\,B_1}{\Gamma^2(1+\mathrm{i}\,\hat\omega/2)} + \frac{\Gamma(-\mathrm{i}\,\hat\omega)\,B_1}{\Gamma^2(1-\mathrm{i}\,\hat\omega/2)}\,(1-\xi^2)^{\mathrm{i}\,\hat\omega} + O(1-\xi^2), \quad \xi^2 \to 1_{-0}, \tag{79}$$

$$\Phi(\xi) = \breve B_2 + \frac{\Gamma(1+\mathrm{i}\,\hat\omega)\,\breve B_1}{2\Gamma^2(1+\mathrm{i}\,\hat\omega/2)} + \frac{\Gamma(1-\mathrm{i}\,\hat\omega)\,\breve B_1}{2\Gamma^2(1-\mathrm{i}\,\hat\omega/2)}\,(\xi^2-1)^{\mathrm{i}\,\hat\omega} + O(\xi^2-1), \quad \xi^2 \to 1_{+0}. \tag{80}$$

As one can see from these formulae, for real $\hat\omega$ solutions contain fast oscillating functions from both sides of a singular point $\xi^2 = 1$, which correspond to B-waves, propagating against the current; these functions, however, remain finite. To match the solutions across

the singular point let us take into consideration a small viscosity in Eq. (1):

$$\frac{\partial u}{\partial t}+\frac{\partial (Uu)}{\partial x}=-g\frac{\partial \eta}{\partial x}+\nu\frac{\partial^2 u}{\partial x^2}, \tag{81}$$

where ν is the coefficient of kinematic viscosity.

Due to this correction to Eq. (1) we obtain the modified Eq. (8) for $\Phi(\xi)$:

$$\nu V^2\frac{d^3\Phi}{d\xi^3}+V\left(1-V^2-\mathrm{i}\,\nu\hat{\omega}\right)\frac{d^2\Phi}{d\xi^2}-\left[\left(1+V^2\right)V'-2\,\mathrm{i}\,\hat{\omega}V^2\right]\frac{d\Phi}{d\xi}+V\hat{\omega}^2\Phi=0. \tag{82}$$

Introducing a new variable $\zeta=\xi^2$ and bearing in mind that $V(\xi)=\xi$ for the accelerating current, we re-write Eq. (82):

$$2\nu\zeta^2\frac{d^3\Phi}{d\zeta^3}+\zeta\left[1-\zeta+(3-\mathrm{i}\,\hat{\omega})\,\nu\right]\frac{d^2\Phi}{d\zeta^2}-\left[\frac{\mathrm{i}\,\nu\hat{\omega}}{2}+(1-\mathrm{i}\,\hat{\omega})\,\zeta\right]\frac{d\Phi}{d\zeta}+\frac{\hat{\omega}^2}{4}\Phi=0. \tag{83}$$

From this equation one can see that in the vicinity of the critical point, where $|\zeta-1|\sim\varepsilon\ll 1$, the viscosity plays an important role, if $\nu\sim\varepsilon^2$. Setting $\nu=\varepsilon^2/2$ and $\zeta=1+\varepsilon z$, we obtain an equation containing the terms up to ε^2:

$$(1+\varepsilon z)^2\frac{d^3\Phi}{dz^3}-(1+\varepsilon z)\left(z-\frac{3-\mathrm{i}\,\hat{\omega}}{2}\varepsilon\right)\frac{d^2\Phi}{dz^2}-\left[(1-\mathrm{i}\,\hat{\omega})(1+\varepsilon z)+\frac{\mathrm{i}\,\hat{\omega}}{4}\varepsilon^2\right]\frac{d\Phi}{dz}+\frac{\varepsilon\hat{\omega}^2}{4}\Phi=0. \tag{84}$$

Looking for a solution to this equation in the form of asymptotic series with respect to parameter ε, $\Phi(z)=\Phi_0(z)+\varepsilon\Phi_1(z)+\ldots$, we obtain in the leading order

$$\frac{d}{dz}\left(\frac{d^2\Phi_0}{dz^2}-z\frac{d\Phi_0}{dz}+\mathrm{i}\,\hat{\omega}\Phi_0\right)=0. \tag{85}$$

Integration of this equation gives the second order equation

$$\frac{d^2\Phi_0}{dz^2}-z\frac{d\Phi_0}{dz}+\mathrm{i}\,\hat{\omega}\left(\Phi_0-D_0\right)=0, \tag{86}$$

where D_0 is a constant of integration.

This equation reduces to the equation of a parabolic cylinder with the help of ansatz $\Phi_0(z)=e^{z^2/4}G(z)+D_0$:

$$\frac{d^2G}{dz^2}+\left(\mathrm{i}\,\hat{\omega}+\frac{1}{2}-\frac{z^2}{4}\right)G=0. \tag{87}$$

Two linearly independent solutions of this equation can be constructed from the following four functions $\mathcal{D}_{\mathrm{i}\hat{\omega}}(\pm z)$ and $\mathcal{D}_{-\mathrm{i}\hat{\omega}-1}(\pm \mathrm{i}z)$ (see [21], 9.255.1). Thus, in the vicinity of the critical point $\xi = 1$ the solution can be presented in the form

$$\Phi_0(z) = D_0 + e^{z^2/4}\left[D_1\mathcal{D}_{\mathrm{i}\hat{\omega}}(z) + D_2\mathcal{D}_{\mathrm{i}\hat{\omega}}(-z)\right], \tag{88}$$

where D_0, D_1, and D_2 are arbitrary constants.

This solution should be matched with the asymptotic expansions (79) and (80) using the following asymptotics of functions of the parabolic cylinder when $|s| \gg 1$ (see [21], 9.246):

$$\mathcal{D}_p(s) \sim s^p\, e^{-s^2/4}{}_2F_0\left(-\frac{p}{2}\,,\frac{1-p}{2}\,;-\frac{2}{s^2}\right), \quad |\arg s| < \frac{3\pi}{4}, \tag{89}$$

$$\mathcal{D}_p(s) \sim s^p\, e^{-s^2/4}{}_2F_0\left(-\frac{p}{2}\,,\frac{1-p}{2}\,;-\frac{2}{s^2}\right) - \frac{\sqrt{2\pi}\, e^{\mathrm{i}\,\pi p}}{\Gamma(-p)} s^{-p-1} e^{s^2/4}{}_2F_0\left(\frac{p}{2}\,,\frac{1+p}{2}\,;\frac{2}{s^2}\right), \tag{90}$$

$$\mathcal{D}_p(s) \sim s^p\, e^{-s^2/4}{}_2F_0\left(-\frac{p}{2}\,,\frac{1-p}{2}\,;-\frac{2}{s^2}\right) - \frac{\sqrt{2\pi}\, e^{-\mathrm{i}\,\pi p}}{\Gamma(-p)} s^{-p-1} e^{s^2/4}{}_2F_0\left(\frac{p}{2}\,,\frac{1+p}{2}\,;\frac{2}{s^2}\right), \tag{91}$$

where Eq. (90) is valid for $\pi/4 < \arg s < 5\pi/4$, and Eq. (91) is valid for $-5\pi/4 < \arg s < -\pi/4$.

With the help of these formulae it is easy to see that the oscillating terms in expansions (79) and (80) should be matched with the last two terms in Eq. (88) which, however, grow infinitely (the former grows, when $z \to -\infty$, and the latter, when $z \to +\infty$). To remove infinitely growing terms from the solution, we need to set $D_1 = D_2 = 0$ in Eq. (88), then after the matching, we obtain in Eqs. (79), (80) and (75), (76)

$$B_1 = \breve{B}_1 = 0, \quad \text{and} \quad B_2 = \breve{B}_2 = D_0. \tag{92}$$

Notice that from the physical point of view the former equality, $B_1 = \breve{B}_1 = 0$, is just a consequence of the fact mentioned in Sec. III that in the trans-critical accelerating current the B-waves (i.e., counter-current propagating waves on the left of critical point and negative-energy waves on the right of it) cannot reach the critical point.

After that assuming that the incident wave arriving from minus infinity has a unit amplitude $A_1 = 1$, using matching conditions (10) and putting $T_p \equiv C_1$, $T_n \equiv C_2$, we obtain

$$B_2\, w_3\left(V_1^2\right) = R + 1, \tag{93}$$

$$B_2\, w_3'(V_1^2) = \frac{-\mathrm{i}\,\hat{\omega} R}{2V_1(1-V_1)} + \frac{\mathrm{i}\,\hat{\omega}}{2V_1(1+V_1)}, \tag{94}$$

$$T_n + T_p = V_2^{\mathrm{i}\hat{\omega}} \breve{w}_3\left(V_2^{-2}\right) \breve{B}_2, \tag{95}$$

$$(V_2+1)T_n - (V_2-1)T_p = \frac{2\mathrm{i}}{\hat{\omega}}\, V_2^{\mathrm{i}\hat{\omega}-2}\left(V_2^2-1\right) \breve{w}_3'\left(V_2^{-2}\right) \breve{B}_2. \tag{96}$$

This set can be readily solved yielding the following transformation coefficients:

$$R = -\frac{w_3'\left(V_1^2\right) - \dfrac{\mathrm{i}\,\hat{\omega}\, w_3\left(V_1^2\right)}{2V_1(1+V_1)}}{w_3'\left(V_1^2\right) + \dfrac{\mathrm{i}\,\hat{\omega}\, w_3\left(V_1^2\right)}{2V_1(1-V_1)}}, \tag{97}$$

$$B_2 = \breve{B}_2 = \frac{R+1}{w_3\left(V_1^2\right)}, \tag{98}$$

$$T_n = \frac{\mathrm{i}}{\hat{\omega}}\, V_2^{\mathrm{i}\hat{\omega}-1}\left(V_2^2-1\right)\left[\frac{\breve{w}_3'\left(V_2^{-2}\right)}{V_2^2} - \frac{\mathrm{i}\,\hat{\omega}}{2}\frac{\breve{w}_3\left(V_2^{-2}\right)}{V_2+1}\right] B_2, \tag{99}$$

$$T_p = -\frac{\mathrm{i}}{\hat{\omega}}\, V_2^{\mathrm{i}\hat{\omega}-1}\left(V_2^2-1\right)\left[\frac{\breve{w}_3'\left(V_2^{-2}\right)}{V_2^2} + \frac{\mathrm{i}\,\hat{\omega}}{2}\frac{\breve{w}_3\left(V_2^{-2}\right)}{V_2-1}\right] B_2. \tag{100}$$

In the long-wave approximation, $\hat{\omega} \to 0$, we obtain (see Appendix C):

$$R = \frac{1-V_1}{1+V_1}, \quad T_p = \frac{V_2+1}{V_1+1}, \quad T_n = -\frac{V_2-1}{V_1+1}, \quad K_{Tp,n} = \frac{V_1}{V_2}\left(\frac{V_2 \pm 1}{V_1+1}\right)^2, \tag{101}$$

where in the last formula sign plus pertains to the positive- and sign minus – to the negative-energy transmitted wave.

These values are purely real, $R > 0$ and $T_p > 0$, whereas $T_n < 0$. The problem of surface wave transformation in a duct with the stepwise change of cross-section and velocity profile is undetermined for such current, therefore in Ref. [15] one of the parameters, R_η – the reflection coefficient in terms of free surface perturbation, was undefined. Now from Eq. (101) it follows that the transformation coefficients in terms of free surface perturbation in Ref. [15] are $R_\eta = T_{p\eta} = -T_{n\eta} = 1$ (for the relationships between the transformation coefficients in terms of velocity potential and free surface perturbation see Appendix A).

Because of the relationships between the coefficients (92), the solution in the domain $\xi_1 < \xi < \xi_2$ is described by the same analytical function $w_3\left(\xi^2\right) \equiv \xi^{\mathrm{i}\hat{\omega}} \breve{w}_3\left(\xi^{-2}\right)$ (see Eqs. (9) and (11) in §6.4 of the book [18]). In the result, the energy flux is still conserved despite a

small viscosity in the vicinity of the critical point $\xi = 1$:

$$J = \frac{2\hat{\omega}}{V_1}\left(1 - |R|^2\right) = \frac{2\hat{\omega}}{V_2}\left(|T_p|^2 - |T_n|^2\right) > 0 \quad \text{or} \quad V_2\left(1 - |R|^2\right) = V_1\left(|T_p|^2 - |T_n|^2\right). \quad (102)$$

As one can see from these expressions, the energy flux in the reflected wave by modulus is always less than in the incident wave, therefore over-reflection here is not possible. In the meantime the energy transmission factors $K_{Tp,n}$ can be greater than 1; this implies that the over-transmission can occur with respect to both positive- and negative-energy waves.

The transformation coefficients $|R|$, $|T_p|$ and $|T_n|$ together with the intermediate coefficients of wave excitation in the transient zone, $|B_2| = |\breve{B}_2|$, are presented in Fig. 9 as functions of dimensionless frequency $\hat{\omega}$ for the particular values of speed, $V_1 = 0.1$ and $V_2 = 1.9$. Qualitatively similar graphics were obtained for other values of V_1 and V_2.

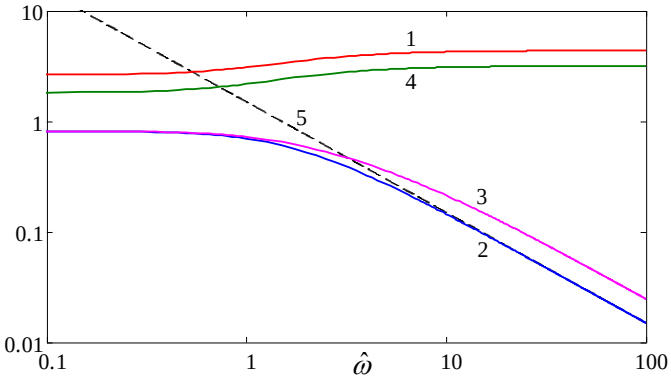


FIG. 9. (color online) Modules of the transformation coefficient as functions of dimensionless frequency $\hat{\omega}$ for $V_1 = 0.1$, $V_2 = 1.9$. Line 1 – $|T_p|$, line 2 – $|T_n|$, line 3 – $|R|$, line 4 – $|B_2| = |\breve{B}_2|$. Dashed line 5 represents the asymptotic for $|T_n| \sim \hat{\omega}^{-1}$.

Notice that both the transmission coefficient of negative energy wave $|T_n|$ and reflection coefficient of positive energy wave $|R|$ decay asymptotically with the same rate $\sim \hat{\omega}^{-1}$.

Figure 10 illustrates the dependences of energy transmission factors on the frequency for two cases: (i) when both $K_{Tp,n} < 1$ ($V_1 = 0.1$, $V_2 = 1.9$) and (ii) when both $K_{Tp,n} > 1$ in a certain range of frequencies $\hat{\omega} < \hat{\omega}_c$ ($V_1 = 0.9$, $V_2 = 8.0$).

In Fig. 11 we present graphics of $|\Phi(\xi)|$ as per Eqs. (74)–(77) for $A_1 = 1$, $A_2 = R$ as per Eq. (97), $D_1 = T_n$ as per Eq. (99), and $D_2 = T_p$ as per Eq. (100). Coefficients $B_1 = \breve{B}_1 = 0$ as per Eq. (92), and $B_2 = \breve{B}_2$ are given by Eq. (98). Line 1 in this figure pertains to the case when $V_1 = 0.1$, $V_2 = 1.9$, and line 2 – to the case when $V_1 = 0.9$, $V_2 = 8.0$.

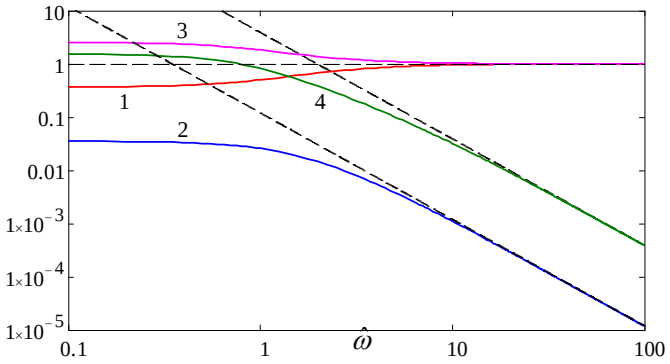


FIG. 10. (color online) The dependences of energy transmission factors on the frequency (i) when both $K_{Tp} < 1$ (line 1) and $K_{Tn} < 1$ (line 2) (here $V_1 = 0.1$, $V_2 = 1.9$); and (ii) when both $K_{Tp} > 1$ (line 3) and $K_{Tn} > 1$ (line 4) in a certain range of frequencies $\hat{\omega} < \hat{\omega}_c$ (here $V_1 = 0.9$, $V_2 = 8.0$). Inclined dashed lines show the asymptotic dependences $K_{Tn} \sim \hat{\omega}^{-2}$.

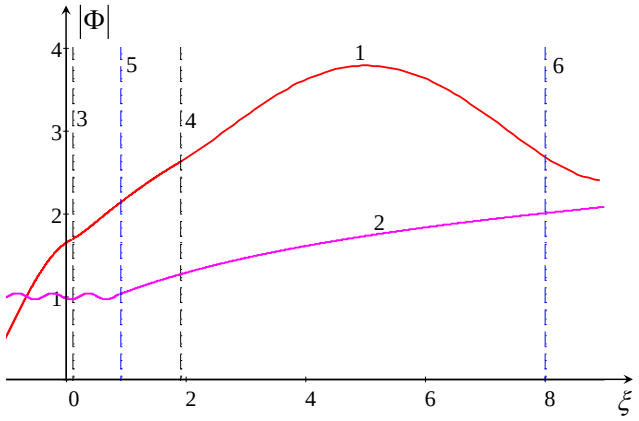


FIG. 11. (color online) Modules of function $\Phi(\xi)$ for wave scattering in accelerating trans-critical current with $V_1 = 0.1$ and $V_2 = 1.9$ (line 1) and $V_1 = 0.9$ and $V_2 = 8.0$ (line 2). Dashed vertical lines 3 and 4 show the transition zone where the current accelerates from $V_1 = 0.1$ to $V_2 = 1.9$, and dashed vertical lines 5 and 6 show the transition zone where the current accelerates from $V_1 = 0.9$ to $V_2 = 8.0$. The plot was generated for $\hat{\omega} = 1$.

D. Wave transformation in trans-critical decelerating currents $V_1 > 1 > V_2 > 0$

In this subsection we consider the wave transformation in gradually decelerating background current assuming that the current is super-critical in the left domain and sub-critical in the right domain. For the sake of simplification of hypergeometric functions used below we chose again the coordinate frame such as shown in Fig. 1b). In such a current the transition

through the critical point, where $V(\xi) = 1$, occurs at $\xi = -1$.

In the left domain, where the current is super-critical, only downstream propagating waves can exist, with the positive or negative energy. In contrast to that, in the right domain, where the background current is sub-critical, two waves of positive energy can coexist; one of them is co-current propagating and another one is counter-current propagating.

The general solution of Eq. (8) in the different domains can be formally presented with the help of functions $\tilde{w}$ as per Eq. (22) and $\hat{w}$ as per Eq. (53):

$$\Phi(\xi) = A_1 e^{\mathrm{i}\,\kappa_1(\xi-\xi_1)} + A_2 e^{\mathrm{i}\,\kappa_2(\xi-\xi_1)}, \qquad \xi < \xi_1, \tag{103}$$

$$\Phi(\xi) = (-\xi)^{-\mathrm{i}\,\hat{\omega}} \left[\hat{B}_1\,\hat{w}_1\left(\xi^{-2}\right) + \hat{B}_2\,\hat{w}_3\left(\xi^{-2}\right)\right], \quad \xi_1 < \xi < -1, \tag{104}$$

$$\Phi(\xi) = B_1\,\tilde{w}_2\left(\xi^2\right) + B_2\,\tilde{w}_3\left(\xi^2\right), \qquad -1 < \xi < \xi_2 < 0, \tag{105}$$

$$\Phi(\xi) = C_1\,e^{\mathrm{i}\,\kappa_3(\xi-\xi_2)} + C_2\,e^{-\mathrm{i}\,\kappa_4(\xi-\xi_2)}, \qquad \xi > \xi_2, \tag{106}$$

where $\kappa_1 = \hat{\omega}/(V_1+1)$, $\kappa_2 = \hat{\omega}/(V_1-1)$, $\kappa_3 = \hat{\omega}/(1+V_2)$, $\kappa_4 = \hat{\omega}/(1-V_2)$.

The matching conditions at $\xi = \xi_1$ provide (cf. Eqs. (55)and (56)):

$$A_1 + A_2 = V_1^{-\mathrm{i}\,\hat{\omega}}\left[\hat{B}_1\,\hat{w}_1\left(V_1^{-2}\right) + \hat{B}_2\,\hat{w}_3\left(V_1^{-2}\right)\right], \tag{107}$$

$$(V_1-1)A_1 - (V_1+1)A_2 = \frac{2\mathrm{i}}{\hat{\omega}}\,V_1^{-\mathrm{i}\,\hat{\omega}-2}\left(V_1^2-1\right)\left[\hat{B}_1\,\hat{w}_1'\left(V_1^{-2}\right) + \hat{B}_2\,\hat{w}_3'\left(V_1^{-2}\right)\right], \tag{108}$$

And similarly the matching conditions at $\xi = \xi_2$ provide:

$$C_1 + C_2 = B_1\,\tilde{w}_2\left(V_2^2\right) + B_2\,\tilde{w}_3\left(V_2^2\right), \tag{109}$$

$$(1-V_2)C_1 - (1+V_2)C_2 = \frac{2\mathrm{i}}{\hat{\omega}}\,V_2\left(1-V_2^2\right)\left[B_1\,\tilde{w}_2'\left(V_2^2\right) + B_2\,\tilde{w}_3'\left(V_2^2\right)\right]. \tag{110}$$

With the help of Eq. (78) we find the asymptotic expansions when $\xi \to -1_{\pm 0}$

$$\Phi(\xi) = \hat{B}_2 + \frac{\Gamma(1-\mathrm{i}\,\hat{\omega})\,\hat{B}_1}{2\Gamma^2(1-\mathrm{i}\,\hat{\omega}/2)} + \frac{\Gamma(1+\mathrm{i}\,\hat{\omega})\,\hat{B}_1}{2\Gamma^2(1+\mathrm{i}\,\hat{\omega}/2)}\,\left(\xi^2-1\right)^{-\mathrm{i}\,\hat{\omega}} + O\left(\xi^2-1\right), \quad \xi \to -1_{-0}, \tag{111}$$

$$\Phi(\xi) = B_2 + \frac{\Gamma(-\mathrm{i}\,\hat{\omega})\,B_1}{\Gamma^2(1-\mathrm{i}\,\hat{\omega}/2)} + \frac{\Gamma\left(\mathrm{i}\,\hat{\omega}\right)\,B_1}{\Gamma^2(1+\mathrm{i}\,\hat{\omega}/2)}\,\left(1-\xi^2\right)^{-\mathrm{i}\,\hat{\omega}} + O\left(1-\xi^2\right), \quad \xi \to -1_{+0}. \tag{112}$$

which are similar to Eqs. (79) and (80), and contain fast oscillating terms corresponding to counter-current propagating B-waves as well.

To match solutions in the vicinity of critical point $\xi = -1$, we again take into consideration a small viscosity. Bearing in mind that $V(\xi) = -\xi$ (see Fig. 1b)) and setting $\zeta = \xi^2 = 1+\varepsilon z$, $\nu = \varepsilon^2/2$, we arrive at the equation similar to Eq. (84):

$$(1+\varepsilon z)^2 \frac{d^3\Phi}{dz^3} + (1+\varepsilon z)\left(z + \frac{3+\mathrm{i}\,\hat{\omega}}{2}\varepsilon\right)\frac{d^2\Phi}{dz^2} + \left[(1+\mathrm{i}\,\hat{\omega})(1+\varepsilon z) + \frac{\mathrm{i}\,\hat{\omega}}{4}\varepsilon^2\right]\frac{d\Phi}{dz} - \frac{\varepsilon\hat{\omega}^2}{4}\Phi = 0. \tag{113}$$

This equation in the leading order on the small parameter $\varepsilon \ll 1$ reduces to (cf. Eq. (85)):

$$\frac{d}{dz}\left(\frac{d^2\Phi_0}{dz^2} + z\frac{d\Phi_0}{dz} + \mathrm{i}\,\hat{\omega}\Phi_0\right) = 0. \tag{114}$$

Integrating this equation and substituting $\Phi_0(z) = D_0 + e^{-z^2/4}G(z)$, we obtain again the equation of a parabolic cylinder in the form (cf. Eq. (115)):

$$\frac{d^2G}{dz^2} + \left(\mathrm{i}\,\hat{\omega} - \frac{1}{2} - \frac{z^2}{4}\right)G = 0. \tag{115}$$

Thus, the general solution to Eq. (114) in the vicinity of critical point $\xi = -1$ can be presented as:

$$\Phi_0(z) = D_0 + e^{-z^2/4}\left[D_1\mathcal{D}_{\mathrm{i}\,\hat{\omega}-1}(z) + D_2\mathcal{D}_{\mathrm{i}\,\hat{\omega}-1}(-z)\right],$$

where D_0, D_1 and D_2 are arbitrary constants.

The asymptotic expansions (89)–(91) show that this solution remains limited for any arbitrary constants. Moreover, the oscillatory terms in Eqs. (111) and (112) become exponentially small after transition through the critical point $\xi = -1$. As was explained in Sec. III, this means that the B-waves running toward the critical point both from the left (negative-energy waves) and from the right (counter-current propagating positive-energy waves) dissipate in the vicinity of the critical point. For this reason the wave energy flux does not conserve in the decelerating trans-critical currents (see Eqs. (127) and (134) below). Taking this fact into account, one can match solutions (111) and (112):

$$D_0 = \frac{\Gamma(-\mathrm{i}\,\hat{\omega})}{\Gamma^2(1-\mathrm{i}\,\hat{\omega}/2)}B_1 + B_2 = \frac{\Gamma(1-\mathrm{i}\,\hat{\omega})}{2\Gamma^2(1-\mathrm{i}\,\hat{\omega}/2)}\hat{B}_1 + \hat{B}_2. \tag{116}$$

After that using the identity $\Gamma(x)\Gamma(1-x) = \pi/\sin\pi x$, we find for the constants D_1 and D_2 the following expressions:

$$D_1 = \frac{-\mathrm{i}\sqrt{\pi/2}}{\Gamma^2(1+\mathrm{i}\hat{\omega}/2)}\frac{e^{-\mathrm{i}\hat{\omega}\ln\varepsilon}}{\sinh\pi\hat{\omega}}B_1, \quad D_2 = \frac{\hat{\omega}\sqrt{\pi/2}}{2\Gamma^2(1+\mathrm{i}\hat{\omega}/2)}\frac{e^{-\mathrm{i}\hat{\omega}\ln\varepsilon}}{\sinh\pi\hat{\omega}}\hat{B}_1. \tag{117}$$

Using the prepared formulae we can now calculate the transformation coefficients for incident waves of either positive or negative energy travelling in the duct from the minus to plus infinity.

1. Transformation of downstream propagating positive-energy wave

Assume first that the incident wave of unit amplitude has positive energy and let us set in Eqs. (103) and (106) $A_1 = 1$, $A_2 = 0$, $C_1 \equiv T_1$, and $C_2 = 0$. Then from Eqs. (107) and (108) we obtain (cf. Eqs. (55) and (56)):

$$\hat{B}_1\,\hat{w}_1\left(V_1^{-2}\right) + \hat{B}_2\,\hat{w}_3\left(V_1^{-2}\right) = V_1^{\mathrm{i}\,\hat{\omega}}, \tag{118}$$

$$\hat{B}_1\,\hat{w}_1'\left(V_1^{-2}\right) + \hat{B}_2\,\hat{w}_3'\left(V_1^{-2}\right) = -\frac{\mathrm{i}\,\hat{\omega}}{2}\frac{V_1^{\mathrm{i}\,\hat{\omega}+2}}{V_1+1}. \tag{119}$$

From this set of equations using the Wronskian (54), one can find

$$\hat{B}_1 = -\frac{\Gamma(\mathrm{i}\,\hat{\omega}/2)\,\Gamma(1+\mathrm{i}\,\hat{\omega}/2)}{\Gamma(1+\mathrm{i}\,\hat{\omega})}\,V_1^{-\mathrm{i}\,\hat{\omega}-2}\left(V_1^2-1\right)^{\mathrm{i}\,\hat{\omega}+1}\left[\frac{\hat{w}_3'\left(V_1^{-2}\right)}{V_1^2} + \frac{\mathrm{i}\,\hat{\omega}}{2}\frac{\hat{w}_3\left(V_1^{-2}\right)}{V_1+1}\right], \tag{120}$$

$$\hat{B}_2 = \frac{\Gamma(\mathrm{i}\,\hat{\omega}/2)\,\Gamma(1+\mathrm{i}\,\hat{\omega}/2)}{\Gamma(1+\mathrm{i}\,\hat{\omega})}\,V_1^{-\mathrm{i}\,\hat{\omega}-2}\left(V_1^2-1\right)^{\mathrm{i}\,\hat{\omega}+1}\left[\frac{\hat{w}_1'\left(V_1^{-2}\right)}{V_1^2} + \frac{\mathrm{i}\,\hat{\omega}}{2}\frac{\hat{w}_1\left(V_1^{-2}\right)}{V_1+1}\right]. \tag{121}$$

Similarly from the matching conditions (109) and (110) we obtain

$$B_1\,\tilde{w}_2\left(V_2^2\right) + B_2\,\tilde{w}_3\left(V_2^2\right) = T_1, \tag{122}$$

$$B_1\,\tilde{w}_2'\left(V_2^2\right) + B_2\,\tilde{w}_3'\left(V_2^2\right) = \frac{-\mathrm{i}\,\hat{\omega}T_1}{2V_2(1+V_2)}. \tag{123}$$

Using the Wronskian (23), we derive from these equations

$$B_1 = -\frac{\Gamma^2(1+\mathrm{i}\,\hat{\omega}/2)}{\Gamma(1+\mathrm{i}\,\hat{\omega})}\left(1-V_2^2\right)^{\mathrm{i}\,\hat{\omega}+1}\left[\tilde{w}_3'\left(V_2^2\right) + \frac{\mathrm{i}\,\hat{\omega}}{2}\frac{\tilde{w}_3\left(V_2^2\right)}{V_2(1+V_2)}\right]T_1, \tag{124}$$

$$B_2 = \frac{\Gamma^2(1+\mathrm{i}\,\hat{\omega}/2)}{\Gamma(1+\mathrm{i}\,\hat{\omega})}\left(1-V_2^2\right)^{\mathrm{i}\,\hat{\omega}+1}\left[\tilde{w}_2'\left(V_2^2\right) + \frac{\mathrm{i}\,\hat{\omega}}{2}\frac{\tilde{w}_2\left(V_2^2\right)}{V_2(1+V_2)}\right]T_1. \tag{125}$$

Substituting B_1 and B_2, as well as $\hat{B}_1$ and $\hat{B}_2$, in Eq. (116), we obtain the transmission coefficient

$$T_1 = -\frac{2\mathrm{i}}{\hat{\omega}}\,V_1^{-\mathrm{i}\,\hat{\omega}-2}\left(\frac{V_1^2-1}{1-V_2^2}\right)^{\mathrm{i}\,\hat{\omega}+1} \times$$

$$\frac{\hat{w}_1'\left(V_1^{-2}\right)}{V_1^2}+\frac{\mathrm{i}\,\hat{\omega}}{2}\frac{\hat{w}_1\left(V_1^{-2}\right)}{V_1+1}-\frac{\Gamma(1-\mathrm{i}\,\hat{\omega})}{2\Gamma^2(1-\mathrm{i}\,\hat{\omega}/2)}\left[\frac{\hat{w}_3'(V_1^{-2})}{V_1^2}+\frac{\mathrm{i}\,\hat{\omega}}{2}\frac{\hat{w}_3\left(V_1^{-2}\right)}{V_1+1}\right]$$
$$\tilde{w}_2'\left(V_2^2\right)+\frac{\mathrm{i}\,\hat{\omega}}{2}\frac{\tilde{w}_2\left(V_2^2\right)}{V_2(1+V_2)}-\frac{\Gamma(-\mathrm{i}\,\hat{\omega})}{\Gamma^2(1-\mathrm{i}\,\hat{\omega}/2)}\left[\tilde{w}_3'\left(V_2^2\right)+\frac{\mathrm{i}\,\hat{\omega}}{2}\frac{\tilde{w}_3\left(V_2^2\right)}{V_2(1+V_2)}\right]. \tag{126}$$

Calculations of the energy fluxes on each side of the transient domain show that they are both positive, but generally different, i.e., the energy flux does not conserve,

$$J_1=J(\xi<-1)=\frac{2\hat{\omega}}{V_1}\ \neq\ J_2=J(\xi>-1)=\frac{2\hat{\omega}}{V_2}\,|T_1|^2. \tag{127}$$

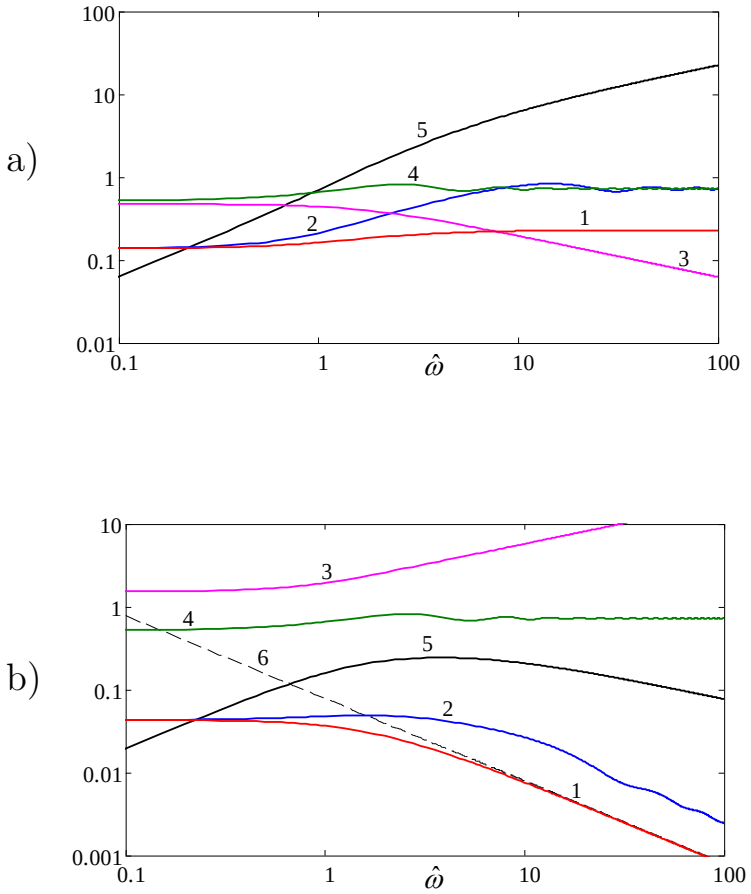


FIG. 12. (color online) Modules of the transmission coefficients $|T_1|$ (line 1 in panel a) and $|T_2|$ (line 1 in panel b), as well as coefficients of wave excitation in the transient domain, $|B_1|$ (line 2), $|B_2|$ (line 3), $|\hat{B}_1|$ (line 4), and $|\hat{B}_2|$ (line 5), for the scattering of positive energy wave (panel a) and negative energy wave (panel b) as functions of dimensionless frequency $\hat{\omega}$ for $V_1=1.9$, $V_2=0.1$. Dashed line 6 in panel (b) represents the high-frequency asymptotic for $|T_2|\sim\hat{\omega}^{-1}$.

This interesting fact can be explained by the partial wave absorption in the critical point

due to viscosity. The detailed explanation of this is given in Section V. The difference in the energy flux in the incident and transmitted waves is independent of the viscosity, when $\nu \to 0$:

$$\Delta J \equiv J_1 - J_2 = 2\hat{\omega}\left(1/V_1 - |T_1|^2/V_2\right) \overset{\hat{\omega}\to 0}{\longrightarrow} \frac{1 - V_1V_2}{V_1(1+V_2)^2}(V_1 - V_2)J_1, \tag{128}$$

and it is easily seen that it can be both positive and negative.

In Fig. 12a) we present the transmission coefficient $|T_1|$ together with the intermediate coefficients of wave excitation in the transient domain, $|B_1|$, $|B_2|$, $|\hat{B}_1|$, and $|\hat{B}_2|$, as functions of dimensionless frequency $\hat{\omega}$ for the particular values of current speed $V_1 = 1.9$ and $V_2 = 0.1$. As one can see from this figure, the transmission coefficient gradually increases with the frequency.

The graphic of $|\Phi(\xi)|$ is shown in Fig. 13 by lines 1 and 2. The plot was generated for $\hat{\omega} = 1$ on the basis of solution Eqs. (103)–(106) with $A_1 = 1$, $A_2 = 0$, $D_1 = T_1$ as per Eq. (126), and $D_2 = 0$. Coefficients B_1 and B_2 are given by Eqs. (124) and (125), and coefficients $\hat{B}_1$ and $\hat{B}_2$ are given by Eqs. (120) and (121). The module of function $\Phi(\xi)$ is discontinuous only in the critical point $\xi = -1$, and the phase of function $\Phi(\xi)$ quickly changes in the small vicinity of this point.

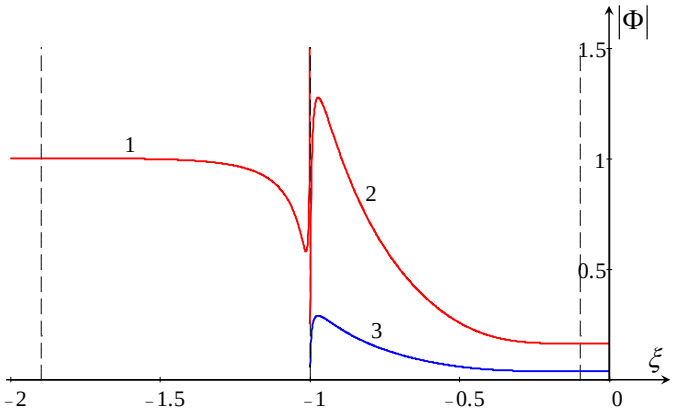


FIG. 13. (color online) Modules of function $\Phi(\xi)$ for wave scattering in decelerating trans-critical current with $V_1 = 1.9$ and $V_2 = 0.1$ for $\hat{\omega} = 1$. Lines 1 and 2 pertain to the scattering of a positive-energy incident wave, and lines 1 and 3 pertain to the scattering of a negative-energy incident wave (line 1 is the same both for positive- and negative-energy waves).

2. Transformation of downstream propagating negative-energy wave

Assume now that the incident wave is a unit amplitude wave of negative energy and correspondingly set $A_1 = 0$, $A_2 = 1$, $C_1 = 0$, and $C_2 \equiv T_2$. Then from Eqs. (107) and (108) we obtain:

$$\hat{B}_1\,\hat{w}_1\left(V_1^{-2}\right) + \hat{B}_2\,\hat{w}_3\left(V_1^{-2}\right) = V_1^{\mathrm{i}\,\hat{\omega}}, \tag{129}$$

$$\hat{B}_1\,\hat{w}_1'\left(V_1^{-2}\right) + \hat{B}_2\,\hat{w}_3'\left(V_1^{-2}\right) = \frac{\mathrm{i}\,\hat{\omega}}{2}\frac{V_1^{\mathrm{i}\,\hat{\omega}+2}}{V_1-1}. \tag{130}$$

From this set we find

$$\hat{B}_1 = -\frac{\Gamma(\mathrm{i}\,\hat{\omega}/2)\,\Gamma(1+\mathrm{i}\,\hat{\omega}/2)}{\Gamma(1+\mathrm{i}\,\hat{\omega})}\,V_1^{-\mathrm{i}\,\hat{\omega}-2}\left(V_1^2-1\right)^{\mathrm{i}\,\hat{\omega}+1}\left[\frac{\hat{w}_3'\left(V_1^{-2}\right)}{V_1^2} - \frac{\mathrm{i}\,\hat{\omega}}{2}\frac{\hat{w}_3\left(V_1^{-2}\right)}{V_1-1)}\right], \tag{131}$$

$$\hat{B}_2 = \frac{\Gamma(\mathrm{i}\,\hat{\omega}/2)\,\Gamma(1+\mathrm{i}\,\hat{\omega}/2)}{\Gamma(1+\mathrm{i}\,\hat{\omega})}\,V_1^{-\mathrm{i}\,\hat{\omega}-2}\left(V_1^2-1\right)^{\mathrm{i}\,\hat{\omega}+1}\left[\frac{\hat{w}_1'\left(V_1^{-2}\right)}{V_1^2} - \frac{\mathrm{i}\,\hat{\omega}}{2}\frac{\hat{w}_1\left(V_1^{-2}\right)}{V_1-1)}\right]. \tag{132}$$

From the matching conditions at $\xi = \xi_2$ (see Eqs. (109) and (110)) we obtain the similar expressions for the coefficients B_1 and B_2 as in Eqs. (124) and (125) with the only replacement of T_1 by T_2. Substituting then all four coefficients B_1, B_2, $\hat{B}_1$, and $\hat{B}_2$ in Eq. (116), we obtain the transmission coefficient T_2:

$$T_2 = -\frac{2\mathrm{i}}{\hat{\omega}}\,V_1^{-\mathrm{i}\,\hat{\omega}-2}\left(\frac{V_1^2-1}{1-V_2^2}\right)^{\mathrm{i}\,\hat{\omega}+1}\times$$
$$\frac{\dfrac{\hat{w}_1'\left(V_1^{-2}\right)}{V_1^2} - \dfrac{\mathrm{i}\,\hat{\omega}}{2}\dfrac{\hat{w}_1\left(V_1^{-2}\right)}{V_1-1} - \dfrac{\Gamma(1-\mathrm{i}\,\hat{\omega})}{2\Gamma^2(1-\mathrm{i}\,\hat{\omega}/2)}\left[\dfrac{\hat{w}_3'(V_1^{-2})}{V_1^2} - \dfrac{\mathrm{i}\,\hat{\omega}\,\hat{w}_3\left(V_1^{-2}\right)}{2(V_1-1)}\right]}{\tilde{w}_2'\left(V_2^2\right) + \dfrac{\mathrm{i}\,\hat{\omega}}{2}\dfrac{\tilde{w}_2\left(V_2^2\right)}{V_2(1+V_2)} - \dfrac{\Gamma(-\mathrm{i}\,\hat{\omega})}{\Gamma^2(1-\mathrm{i}\,\hat{\omega}/2)}\left[\tilde{w}_3'\left(V_2^2\right) + \dfrac{\mathrm{i}\,\hat{\omega}\,\tilde{w}_3\left(V_2^2\right)}{2V_2(1+V_2)}\right]}. \tag{133}$$

Calculations of the energy fluxes on each side of the transient domain show that they are not equal again, moreover, they have opposite signs in the left and right domains:

$$J_1 = J(\xi<-1) = -\frac{2\hat{\omega}}{V_1} < 0, \quad J_2 = J(\xi>-1) = \frac{2\hat{\omega}}{V_2}\,|T_2|^2 > 0. \tag{134}$$

The wave of negative energy in the left domain propagates to the right, its group velocity V_g is positive, but because it has a negative energy E, its energy flux, $J = EV_g$ is negative.

In the long-wave approximation, $\hat{\omega} \to 0$ we obtain (see Appendix C):

$$T_1 = \frac{V_2(V_1+1)}{V_1(V_2+1)}, \quad T_2 = \frac{V_2(V_1-1)}{V_1(V_2+1)}, \quad K_{T1,T2} = \frac{V_2}{V_1}\left(\frac{V_1\pm 1}{V_2+1}\right)^2, \tag{135}$$

where in the last formula sign plus pertains to the positive- and sign minus – to the negative-energy wave. As one can see, the transmission coefficients are purely real and positive, $T_{1,2} > 0$, in both cases.

The problem of surface wave transformation in a duct with the stepwise change of cross-section and velocity profile is undetermined for such current too; however from the results obtained it follows that in terms of free surface perturbation the transformation coefficients are

$$T_{1\eta} = \frac{V_2}{V_1}\left(\frac{V_1+1}{V_2+1}\right)^2, \quad T_{2\eta} = \frac{V_2}{V_1}\frac{V_1^2-1}{(V_2+1)^2} \tag{136}$$

(for the relationships between the transformation coefficients in terms of velocity potential and free surface perturbation see Appendix A).

In Fig. 12b) we present the transmission coefficient $|T_2|$ together with the coefficients of wave excitation in the intermediate domain, $|B_1|$, $|B_2|$, $|\hat{B}_1|$, and $|\hat{B}_2|$, as functions of dimensionless frequency $\hat{\omega}$ for the particular values of current speed $V_1 = 1.9$ and $V_2 = 0.1$. As one can see from this figure, the transmission coefficient remains almost constant for small frequencies when $\hat{\omega} < 1$, then it decreases with the frequency and asymptotically vanishes as $|T_2| \sim \hat{\omega}^{-1}$ when $\hat{\omega} \to \infty$.

The graphic of $|\Phi(\xi)|$ is shown in Fig. 13 by lines 1 and 3 (the left branch of function $|\Phi(\xi)|$ for the incident negative- and positive-energy waves are the same). The plot was generated for $\hat{\omega} = 1$ on the basis of solution Eqs. (103)–(106) with $A_1 = 0$, $A_2 = 1$, $D_1 = 0$, and $D_2 = T_2$ as per Eq. (133). Coefficients B_1 and B_2 are given by Eqs. (124) and (125), and coefficients $\hat{B}_1$ and $\hat{B}_2$ are given by Eqs. (131) and (132). The module of function $\Phi(\xi)$ is discontinuous only in the critical point $\xi = -1$, but the phase of function $\Phi(\xi)$ quickly changes in the small vicinity of this point.

3. Transformation of a counter-current propagating wave

Consider now the case when the incident wave propagates against the mean current in the spatially variable current from the right domain where the background current is sub-critical. There are no waves capable to propagate against in the $\xi < -1$ domain where $V > 1$, therefore there is no transmitted wave in this case. However, the incident wave can propagate against the current and even penetrate into the transient zone $\xi_1 < \xi < \xi_2$ up to the critical point $\xi = -1$ until the current remains subcritical.

Because there are no waves in the domain $\xi < -1$, we should set in Eqs. (103)–(106) $A_1 = A_2 = \hat{B}_1 = \hat{B}_2 = 0$, $C_1 \equiv R$, and $C_2 = 1$. Then the matching condition (116) yields

$$B_2 = -\frac{\Gamma(-\mathrm{i}\,\hat{\omega})}{\Gamma^2(1-\mathrm{i}\,\hat{\omega}/2)} B_1, \tag{137}$$

and from Eqs. (109) and (110) we obtain for the reflection coefficient

$$R = -\frac{\tilde{w}_2'\left(V_2^2\right) - \dfrac{\mathrm{i}\,\hat{\omega}}{2}\dfrac{\tilde{w}_2\left(V_2^2\right)}{V_2(1-V_2)} - \dfrac{\Gamma(-\mathrm{i}\,\hat{\omega})}{\Gamma^2(1-\mathrm{i}\,\hat{\omega}/2)}\left[\tilde{w}_3'(V_2^2) - \dfrac{\mathrm{i}\,\hat{\omega}}{2}\dfrac{\tilde{w}_3\left(V_2^2\right)}{V_2(1-V_2)}\right]}{\tilde{w}_2'\left(V_2^2\right) + \dfrac{\mathrm{i}\,\hat{\omega}}{2}\dfrac{\tilde{w}_2\left(V_2^2\right)}{V_2(1+V_2)} - \dfrac{\Gamma(-\mathrm{i}\,\hat{\omega})}{\Gamma^2(1-\mathrm{i}\,\hat{\omega}/2)}\left[\tilde{w}_3'\left(V_2^2\right) + \dfrac{\mathrm{i}\,\hat{\omega}}{2}\dfrac{\tilde{w}_3\left(V_2^2\right)}{V_2(1+V_2)}\right]}. \tag{138}$$

Then, from Eqs. (109) and (137) we find B_1 and B_2; in particular for B_1 we obtain:

$$B_1 = \frac{1+R}{\tilde{w}_2\left(V_2^2\right) - \dfrac{\Gamma(-\mathrm{i}\,\hat{\omega})}{\Gamma^2(1-\mathrm{i}\,\hat{\omega}/2)}\tilde{w}_3\left(V_2^2\right)}. \tag{139}$$

Graphics of modulus of reflection coefficient $|R|$ as well as coefficients $|B_1|$ and $|B_2|$ are shown in Fig. 14 as functions of dimensionless frequency $\hat{\omega}$ for the particular values of $V_1 = 1.9$ and $V_2 = 0.1$.

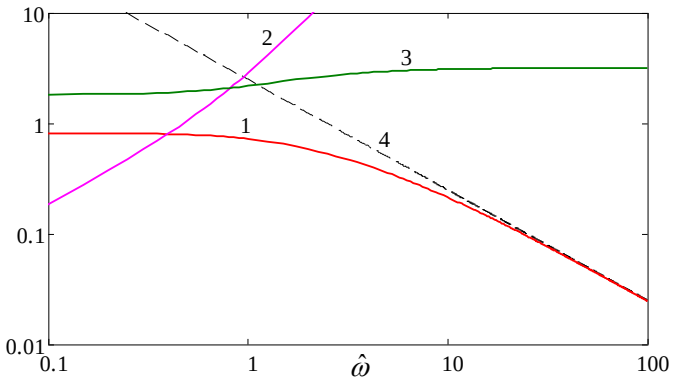


FIG. 14. (color online) Modulus of the reflection coefficients $|R|$ (line 1) and coefficients of wave excitation in the transient domain, $|B_1|$ (line 2) and $|B_2|$ (line 3), as functions of dimensionless frequency $\hat{\omega}$ for $V_1 = 1.9$, $V_2 = 0.1$. Dashed line 4 represents the high-frequency asymptotic for $|R| \sim \hat{\omega}^{-1}$.

In the long-wave approximation, $\hat{\omega} \to 0$, using the asymptotics of hypergeometric function ${}_2F_1(a, b; c; d)$ (see Appendix C), we obtain the limiting value of the reflection coefficient

$$R = \frac{1-V_2}{1+V_2}. \tag{140}$$

In terms of free surface perturbation this value corresponds to $R_\eta = 1$ (for the relationships between the transformation coefficients in terms of velocity potential and free surface perturbation see Appendix A). This formally agrees with the solution found in Ref. [15].

In Fig. 15 we present graphics of $|\Phi(\xi)|$ as per Eqs. (103)–(106) for $A_1 = A_2 = 0$, $D_1 = 1$, and $D_2 = R$ as per Eq. (138). Coefficients B_1 and B_2 are given by Eqs. (139) and (137), and coefficients $\hat{B}_1 = \hat{B}_2 = 0$. A plot was generated for three dimensionless frequencies: line 1 – for $\hat{\omega} = 0.1$, line 2 – for $\hat{\omega} = 1$, and line 3 – for $\hat{\omega} = 100$. The phase of function $\Phi(\xi)$ infinitely increases when the incident wave approaches the critical point $\xi = -1$.

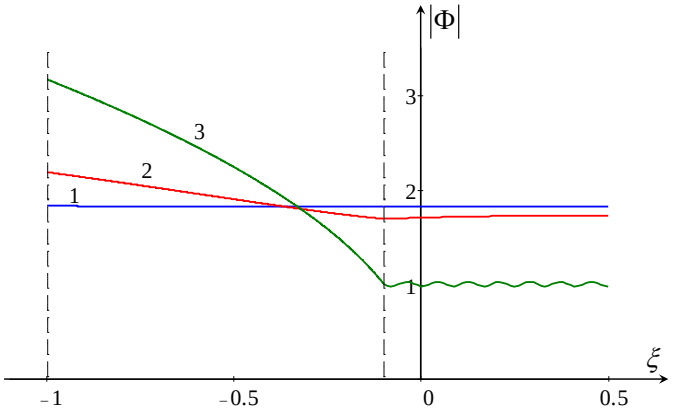


FIG. 15. (color online) Module of function $\Phi(\xi)$ for a counter-current propagating incident wave which scatters in the decelerating trans-critical current with $V_1 = 1.9$ and $V_2 = 0.1$ for the particular values of $\hat{\omega}$: line 1 – $\hat{\omega} = 0.1$, line 2 – $\hat{\omega} = 1$, and line 3 – $\hat{\omega} = 100$.

The energy fluxes in the incident J_i and reflected J_r waves in the right domain ($\xi > \xi_2$) are

$$J_i = -\frac{2\hat{\omega}}{V_2} < 0, \quad J_r = \frac{2\hat{\omega}}{V_2}|R|^2 > 0. \tag{141}$$

Thus, the total energy flux in the right domain $\Delta J \equiv J_i - J_r = -(2\hat{\omega}/V_2)(1 - |R|^2) < 0$ is negative; it transfers towards the critical point, where it is absorbed by the viscosity.

V. DISCUSSION AND CONCLUSION

In this paper we have calculated the transformation coefficients of shallow water gravity waves propagating on a longitudinally varying quasi-one-dimensional current. Owing to the choice of a piece-linear velocity profile $U(x)$ (or, in the dimensionless variables, $V(\xi)$, see Fig. 1) we were able to calculate analytically the scattering coefficients as functions of

incident wave frequency $\hat{\omega}$ for accelerating and decelerating sub-, super-, and trans-critical currents, as well as for all possible types of incident wave.

Presented analysis pertains to the dispersionless case when the wavelengths of all waves participating in the scattering process are much greater than the water depth in the canal. However, the wavelengths λ can be comparable with or even less than the characteristic length of current inhomogeneity L. In the long-wave limit $\lambda \gg L$, the scattering coefficients are expressed through the simple algebraic formulae which are in agreement with the formulae derived in [15] for the case of abrupt change of canal cross-section.

The most important property of scattering processes in sub-, super-, and accelerating trans-critical currents is that the wave energy flux conserves, $J = \text{const}$, (see Eq. (6) and the text below Eq. (8)). This law provides a highly convenient and physically transparent basis for the analysis of wave scattering.

In the simplest case of sub-critical currents ($U(x) < c_0$, or $V(\xi) < 1$), both accelerating and decelerating, all participating waves possess a positive energy, and the energy flux of the unit amplitude incident wave (no matter whether running from the left or from the right) is divided between reflected and transmitted waves in a such manner that $|R|^2 + K_T = 1$ (see Eqs. (34) and (33) for the wave running from the left, and Eqs. (45) and (44) for the wave running from the right).

In super-critical currents ($V(\xi) > 1$) there are positive- and negative-energy waves both propagating downstream but carrying energy fluxes of opposite signs. Propagating through the inhomogeneity domain $\xi_1 < \xi < \xi_2$, they transform into each other in a such way that the energy flux of each wave grows in absolute value to the greater extent the greater the velocity ratio is. As a result, at $\xi > \xi_2$ the energy flux of each transmitted wave can become greater (in absolute value) than that of the incident wave (see Fig. 8). Quantitatively the increase of wave-energy fluxes can be easily estimated in the low-frequency limit using Eqs. (65) and (73).

The scattering process in accelerating trans-critical currents ($V_1 < 1 < V_2$) looks like a hybrid with respect to those in sub- and super-critical currents. The incident wave can be the only co-current propagating wave of positive energy. Initially, at $\xi < \xi_1$, its energy flux (at unit amplitude) $J_0 = 2\hat{\omega}/V_1$, but in the domain $\xi_1 < \xi < 1$ it partially transforms into the counter-current propagating reflected wave, and at $\xi = 1$ its energy flux is only $J_0(1 - |R|^2)$ (see Eq. (102)). Further, in the super-critical domain $1 < \xi < \xi_2$, it generates

a negative-energy wave, and the energy fluxes of both waves grow in absolute value to the greater extent the greater V_2 is. And again this process can be better understand in the low-frequency limit by means of Eqs. (101).

The most interesting scattering processes takes place in decelerating trans-critical currents ($V_1 > 1 > V_2$) where B-waves (which are either counter-current propagating positive-energy waves or downstream propagating negative energy waves, see Sec. III) run to the critical point (where $V(\xi) = 1$) and become highly-oscillating in its vicinity. For this reason we are forced to give up the model of ideal fluid and to take into account an infinitesimal viscosity in the neighborhood of the critical point. As a result, the energy flux continues to conserve on the left and right of the critical point, but changes in its small vicinity. Let us illuminate the details of this phenomenon.

Consider first an incident positive-energy F-wave arriving from the left. In the transient domain $\xi_1 < \xi < -1$ it partially transforms into the negative-energy B-wave. The total wave flux conserves, whereas the energy flux of each individual wave increases in absolute value up to the critical point (to the more greater extent the greater V_1 is). As follows from the qualitative consideration on the basis of JWKB method (see Section III) and from exact analytical solutions (see Subsection IV D), near the critical point the B-wave becomes highly oscillating in space. This causes its absorbtion due to viscosity; as will be shown below, the absorbtion is proportional to ν/λ^2. In contrast to that, the wavelength of the co-current propagating F-wave does not change significantly in the process of transition through the critical point (see Section III), therefore the effect of viscosity onto this wave is negligible. After transition this wave runs through the non-unform subcritical domain $-1 < \xi < \xi_2$ and partially transforms into another B-wave – a counter-current propagating wave of positive energy. This wave approaching the critical point also becomes highly oscillating and therefore absorbs in the vicinity of that point. The energy flux of transmitted F-wave decreases proportional to V_2. The total change of energy flux in transition from the incident to the transmitted wave is described by Eqs. (128), and in the limit $\hat{\omega} \to 0$ is determined by the product $V_1 V_2$.

If the incident wave arriving from minus infinity is the B-wave of negative energy carrying a negative energy flux (see J_1 in Eq. (134)), then in the transient zone, $\xi_1 < \xi < -1$, it generates due to scattering on inhomogeneous current the F-wave of positive energy, so that the wave fluxes of both waves grow in absolute value. The B-wave absorbs due to viscosity

in the vicinity of the critical point $\xi = -1$, whereas the F-wave freely passes through this point with an insignificant change of its wavelength. After passing through the critical point the F-wave generates in the domain $-1 < \xi < \xi_2$ a new B-wave of positive energy, which propagates a counter-current towards the critical point and absorbs in its vicinity due to viscosity. Therefore, the energy flux of the F-wave increases first from zero at $\xi = \xi_1$ up to some maximal value at $\xi = -1$, then it decreases due to transformation of wave energy into the B-wave to some value at $\xi = \xi_2$ (see J_2 in Eq. (134)), and then remains constant. In the long-wave approximation, $\hat{\omega} \to 0$, we obtain

$$\Delta J \equiv |J_2| - |J_1| = \left(\frac{V_1}{V_2}|T_2|^2 - 1\right)|J_1| = \frac{V_2\,|J_1|}{V_1(1+V_2)^2}\left[V_1^2 - V_1\left(4 + V_2 + \frac{1}{V_2}\right) + 1\right].$$

Analysis of this expression shows that because $V_2 + 1/V_2 \geq 2$, then ΔJ can be positive (i.e., the energy flux of transmitted wave can be greater than the energy flux of incident wave by absolute value), if $V_1 > 3 + 2\sqrt{2} \approx 5.83$.

If there are two incident waves arriving simultaneously from minus infinity so that one of them has positive energy and another one – negative energy, then at some relationships between their amplitudes and phases it may happen that in the transient zone in front of the critical point the superposition of these waves and scattered waves generated by them can annihilate either the positive-energy F-wave or negative-energy B-wave. In the former case it will not be a transmitted wave behind the critical point, because the B-wave in its vicinity completely absorbs (the "opacity" phenomena occurs). In the latter case there is no negative-energy B-wave on the left of the critical point and therefore there is nothing to absorb, and the F-wave passes through this point without loss of energy (we assume that the viscosity is negligible). Further, the F-wave spends some portion of its energy transforming into the counter-current propagating B-wave of positive energy which ultimately dissipates in the vicinity of the critical point. Nevertheless, the residual energy flux of transmitted wave at $\xi > \xi_2$ turns to be equal to the total energy flux of two incident waves at $\xi < \xi_1$, and in such a very particular case the energy flux conserves.

Finally, if an incident B-wave of positive energy arrives from plus infinity, then in the inhomogeneous zone, $-1 < \xi < \xi_2$, it generates a co-current propagating F-wave of positive energy. The energy fluxes of both these waves have opposite signs and decrease in absolute value as one approaches the critical point. In the critical point the energy flux of F-wave vanishes, and the remainder of the B-wave absorbs. In this case the less the V_2 the higher the

reflection coefficient $|R|$ is, and this is especially clear in the low-frequency approximation, see Eq. (140).

The analysis presented above is based on the fact that the wavelengths of scattered waves drastically decrease in the vicinity of a critical point, where $V(\xi) = 1$. In such case either the dispersion, or dissipation, or both these effects may enter into play. We will show here that at certain situations the viscosity can predominate over the dispersion. Considering the harmonic solution $\sim e^{\mathrm{i}\kappa\xi}$ of Eq. (82) in the vicinity of a critical point and neglecting the term $\sim V'$, we obtain the dispersion relation extending (11). In the dimensional form it is:

$$(\omega - \mathbf{kU})^2 = c_0^2 k^2 - \mathrm{i}\nu k^2 (\omega - \mathbf{kU}) . \tag{142}$$

The solution to this equation for small a viscosity $\nu k \ll c_0$ is

$$\omega = |c_0 \pm U||\mathbf{k}| - \mathrm{i}\nu k^2/2. \tag{143}$$

The viscosity effect becomes significant when the imaginary and real parts of frequency become of the same order of magnitude. This gives $|\mathbf{k}| \sim 2|c_0 \pm U|/\nu$. Multiplying both sides of this relationship by h, we obtain $|\mathbf{k}|h \sim 2h|c_0 \pm U|/\nu$. For the counter-current propagating B-wave $|c_0 - U| \to 0$, therefore the product $|\mathbf{k}|h$ can be small despite of smallness on ν. So, the condition $|\mathbf{k}|h \sim 2h|c_0 - U|/\nu \ll 1$ allows us to consider the influence of viscosity in the vicinity of a critical point, whereas the dispersion remains negligibly small. In the meantime, the wavelength of co-current propagating F-wave does not change dramatically in the process of transition through the critical point (see Section III). For such wave the viscosity is significant when $|\mathbf{k}|h \sim 2h(c_0 + U)/\nu \gg 1$ which corresponds to the deep-water approximation.

Notice in the conclusion that the wave-current interaction in recent years became a very hot topic due to applications both to the natural processes occurring in the oceans and as a model of physical phenomena closely related with the Hawking radiation in astrophysics [1–5, 9–11]. The influence of high-momentum dissipation on the Hawking radiation was considered in astrophysical application [22] (see also [23] where the dissipative fields in de Sitter and black hole spacetimes metrics were studied with application to the quantum entanglement due to pair production and dissipation). The peculiarity of our paper is in the finding of exactly solvable model which enabled us to construct analytical solutions and calculate the scattering coefficients in the dispersionless limit. We have shown, in particular,

that in the case of accelerating trans-critical current both the reflection coefficient of positive-energy wave and transmission coefficient of negative-energy wave decrease asymptotically with the frequency as $|R| \sim T_n \sim \hat{\omega}^{-1}$. This can be presented in terms of the Hawking temperature $T_H = (1/2\pi)(dU/dx)$ (see, e.g., [3, 10]) and dimensional frequency ω as $|R| \sim T_n \sim 2\pi T_H/\omega$.

ACKNOWLEDGMENTS

This work was initiated when one of the authors (Y.S.) was the invited Visiting Professor at the Institut Pprime, Université de Poitiers in August–October, 2016. Y.S. is very grateful to the University and Region Poitou-Charentes for the invitation and financial support during his visit. Y.S. acknowledges also the funding of this study from the State task programme in the sphere of scientific activity of the Ministry of Education and Science of the Russian Federation (Project No. 5.1246.2017/4.6). The research of A.E. was supported by the Australian Government Research Training Program Scholarship.

Appendix A: Energy Flux Conservation

Let us multiply equation (5) by the complex-conjugate function $\overline{\varphi}$ and subtract from the result complex-conjugate equation:

$$\overline{\varphi}\left(\frac{\partial}{\partial t}+U\frac{\partial}{\partial x}\right)\left(\frac{\partial\varphi}{\partial t}+U\frac{\partial\varphi}{\partial x}\right)-\varphi\left(\frac{\partial}{\partial t}+U\frac{\partial}{\partial x}\right)\left(\frac{\partial\overline{\varphi}}{\partial t}+U\frac{\partial\overline{\varphi}}{\partial x}\right)= c_0^2U\left[\overline{\varphi}\frac{\partial}{\partial x}\left(\frac{1}{U}\frac{\partial\varphi}{\partial x}\right)-\varphi\frac{\partial}{\partial x}\left(\frac{1}{U}\frac{\partial\overline{\varphi}}{\partial x}\right)\right]. \tag{A1}$$

Dividing this equation by U and rearranging the terms we present this equation in the form:

$$\frac{\partial}{\partial t}\left[\frac{\overline{\varphi}}{U}\left(\frac{\partial\varphi}{\partial t}+U\frac{\partial\varphi}{\partial x}\right)-\frac{\varphi}{U}\left(\frac{\partial\overline{\varphi}}{\partial t}+U\frac{\partial\overline{\varphi}}{\partial x}\right)\right]+ \frac{\partial}{\partial x}\left[\overline{\varphi}\left(\frac{\partial\varphi}{\partial t}+U\frac{\partial\varphi}{\partial x}\right)-\varphi\left(\frac{\partial\overline{\varphi}}{\partial t}+U\frac{\partial\overline{\varphi}}{\partial x}\right)-\frac{c_0^2}{U}\left(\overline{\varphi}\frac{\partial\varphi}{\partial x}-\varphi\frac{\partial\overline{\varphi}}{\partial x}\right)\right]=0. \tag{A2}$$

If we denote

$$\mathcal{E} = \frac{\mathrm{i}}{U}\left[\bar{\varphi}\left(\frac{\partial\varphi}{\partial t} + U\frac{\partial\varphi}{\partial x}\right) - \varphi\left(\frac{\partial\bar{\varphi}}{\partial t} + U\frac{\partial\bar{\varphi}}{\partial x}\right)\right], \tag{A3}$$

$$J = \mathcal{E}U - \mathrm{i}\,\frac{c_0^2}{U}\left(\bar{\varphi}\frac{\partial\varphi}{\partial x} - \varphi\frac{\partial\bar{\varphi}}{\partial x}\right), \tag{A4}$$

then Eq. (A2) can be presented in the form of the conservation law

$$\frac{\partial\mathcal{E}}{\partial t} + \frac{\partial J}{\partial x} = 0, \tag{A5}$$

For the waves harmonic in time, $\varphi = \Phi(x)e^{-i\omega t}$, both $\mathcal{E}$ and J do not depend on time, and Eq. (A5) reduces to $J = \text{const}$. Substituting in Eq. (A4) written in the dimensionless form solution (16) for $\xi < \xi_1$ and solution (18) for $\xi > \xi_2$, after simple manipulations we obtain

$$J = \frac{2\hat{\omega}}{V_1}\left(1 - |R|^2\right), \quad \xi < \xi_1; \tag{A6}$$

$$J = \frac{2\hat{\omega}}{V_2}|T|^2, \qquad \xi > \xi_2. \tag{A7}$$

Equating J calculated in Eqs. (A6) and (A7), we obtain the relationship between the transformation coefficients presented in Eq. (34).

Using then solution (17) for $\xi_1 < \xi < \xi_2$, we obtain

$$J = 2\hat{\omega}\left|B_1 w_2(\xi^2) + B_2 w_3(\xi^2)\right|^2 -$$
$$2i(1-\xi^2)\left\{|B_1|^2\left[w_2'(\xi^2)\overline{w_2}(\xi^2) - \overline{w_2'}(\xi^2)w_2(\xi^2)\right] + |B_2|^2\left[w_3'(\xi^2)\overline{w_3}(\xi^2) - \overline{w_3'}(\xi^2)w_3(\xi^2)\right] + \right.$$
$$\left. B_1\overline{B_2}\left[w_2'(\xi^2)\overline{w_3}(\xi^2) - w_2(\xi^2)\overline{w_3'}(\xi^2)\right] - \overline{B_1}B_2\left[\overline{w_2'}(\xi^2)w_3(\xi^2) - \overline{w_2}(\xi^2)w_3'(\xi^2)\right]\right\} = \text{const}. \tag{A8}$$

It was confirmed by direct calculations with the solutions (16)–(18) that J is indeed independent of ξ for given other parameters.

In a similar way, for the super-critical accelerating current one can obtain in the intermediate interval $\xi_1 < \xi < \xi_2$

$$J = \frac{2\hat{\omega}}{\xi^2}\left|B_1\breve{w}_1(\xi^{-2}) + B_2\breve{w}_3(\xi^{-2})\right|^2 - \frac{2\mathrm{i}\,(\xi^2-1)}{\xi^4}\left\{|B_1|^2\left[\breve{w}_1'(\xi^{-2})\overline{\breve{w}_1}(\xi^{-2}) - \overline{\breve{w}_1'}(\xi^{-2})\breve{w}_1(\xi^{-2})\right] + \right.$$
$$|B_2|^2\left[\breve{w}_3'(\xi^{-2})\overline{\breve{w}_3}(\xi^{-2}) - \overline{\breve{w}_3'}(\xi^{-2})\breve{w}_3(\xi^{-2})\right] + B_1\overline{B_2}\left[\breve{w}_1'(\xi^{-2})\overline{\breve{w}_3}(\xi^{-2}) - \breve{w}_1(\xi^{-2})\overline{\breve{w}_3'}(\xi^{-2})\right] -$$
$$\left.\overline{B_1}B_2\left[\overline{\breve{w}_1'}(\xi^{-2})\breve{w}_3(\xi^{-2}) - \overline{\breve{w}_1}(\xi^{-2})\breve{w}_3'(\xi^{-2})\right]\right\} = \text{const}. \tag{A9}$$

Here the coefficients B_1 and B_2 should be taken either from Eqs. (59) and (60) for the scattering of positive energy wave or from Eqs. (68) and (69) for the scattering of negative energy wave.

The transformation coefficients R and T were derived in this paper in terms of the velocity potential φ. But they can be also presented in terms of elevation of a free surface η. Using Eq. (4) for $x < x_1$ and definition of φ just after that equation we obtain for a wave sinusoidal in space

$$(\omega - \mathbf{k}\cdot\mathbf{U_1})\eta = khu = \mathrm{i}hk^2\varphi. \tag{A10}$$

Bearing in mind that according to the dispersion relation $\omega - \mathbf{k}\cdot\mathbf{U_1} = c_0|k|$, we find from Eq. (A10)

$$\varphi = -\mathrm{i}\frac{c_0}{h|k|}\eta = -\mathrm{i}\frac{c_0(c_0 \pm U_1)}{h\omega}\eta, \tag{A11}$$

where sign plus pertains to co-current propagating incident wave and sign minus – to counter-current propagating reflected wave.

Similarly for the transmitted wave for $x > x_2$ we derive

$$\varphi = -\mathrm{i}\frac{c_0(c_0 + U_2)}{h\omega}\eta. \tag{A12}$$

Substitute expressions (A11) and (A12) for incident, reflected and transmitted waves into Eq. (34) and bear in mind that $R \equiv \varphi_r/\varphi_i$, $T \equiv \varphi_t/\varphi_i$, and ω and c_0 are constant parameters:

$$V_2\left[(1+V_1)^2 - (1-V_1)^2\,|R_\eta|^2\right] = V_1\,(1+V_2)^2\,|T_\eta|^2, \tag{A13}$$

where

$$R_\eta \equiv \frac{\eta_r}{\eta_i} = \frac{1+V_1}{1-V_1}R, \quad \text{and} \quad T_\eta \equiv \frac{\eta_t}{\eta_i} = \frac{1+V_1}{1+V_2}T. \tag{A14}$$

In such form Eq. (34) represents exactly the conservation of energy flux (see [14, 15]).

Appendix B: Derivation of Matching Conditions for Equation (8)

To derive the matching conditions in the point ξ_1, let us present Eq. (8) in two equivalent forms:

$$\left[\left(V - \frac{1}{V}\right)\Phi\right]'' - \left[\left(1 + \frac{1}{V^2}\right)V'\Phi\right]' - 2\,\mathrm{i}\,\hat{\omega}\,\Phi' - \frac{\hat{\omega}^2}{V}\,\Phi = 0. \tag{B1}$$

$$\left[\left(V - \frac{1}{V}\right)\Phi'\right]' - 2\,\mathrm{i}\,\hat{\omega}\,\Phi' - \frac{\hat{\omega}^2}{V}\,\Phi = 0, \tag{B2}$$

Let us multiply now Eq. (B2) by $\zeta = \xi - \xi_1$ and integrate it by parts with respect to ζ from $-\varepsilon$ to ε:

$$\left\{\zeta\left[\left(V-\frac{1}{V}\right)\Phi' - 2\,\mathrm{i}\,\hat{\omega}\,\Phi\right] - \left(V-\frac{1}{V}\right)\Phi\right\}\Big|_{-\varepsilon}^{\varepsilon} + \int_{-\varepsilon}^{\varepsilon}\left[\left(1+\frac{1}{V^2}\right)V' + 2\,\mathrm{i}\,\hat{\omega} - \frac{\hat{\omega}^2}{V}\,\zeta\right]\Phi\,d\zeta = 0. \tag{B3}$$

In accordance with our assumption about the velocity, function $V(\zeta)$ is piece-linear, and its derivative is piece-constant. Assuming that function $\Phi(\zeta)$ is limited on the entire ζ-axis, $|\Phi| \le M$, where $M < \infty$ is a constant, we see that the integral term vanishes when $\varepsilon \to 0$. The very first term, which contains ζ in front of the curly brackets $\{\ldots\}$, also vanishes when $\varepsilon \to 0$, and we have

$$\left[\left(V-\frac{1}{V}\right)\Phi\right]\Big|_{-\varepsilon}^{\varepsilon} = 0. \tag{B4}$$

This implies that $\Phi(\zeta)$ is a continuous function in the point $\zeta = \zeta_1$.

If we integrate then Eq. (B1) with respect to ζ in the same limits as above, we obtain:

$$\left[\left(V-\frac{1}{V}\right)\Phi' - 2\,\mathrm{i}\,\hat{\omega}\,\Phi\right]\Big|_{-\varepsilon}^{\varepsilon} - \hat{\omega}^2\int_{-\varepsilon}^{\varepsilon}\frac{\Phi(\zeta)}{V(\zeta)}\,d\zeta = 0. \tag{B5}$$

Under the same assumptions about functions $V(\zeta)$ and $\Phi(\zeta)$, the integral term here vanishes when $\varepsilon \to 0$ and we obtain:

$$\left[\left(V-\frac{1}{V}\right)\Phi' - 2\,\mathrm{i}\,\hat{\omega}\,\Phi\right]_{-\varepsilon} = \left[\left(V-\frac{1}{V}\right)\Phi' - 2\,\mathrm{i}\,\hat{\omega}\,\Phi\right]_{\varepsilon}. \tag{B6}$$

Due to continuity of functions $V(\zeta)$ and $\Phi(\zeta)$ in the point $\zeta = \zeta_1$, we conclude that the derivative $\Phi'(\zeta)$ is a continuous function in this point too. The same matching conditions can be derived for the point ξ_2 as well.

Appendix C: The Transformation Coefficients in the Long-Wave Limit

The long-wave approximation in the dispresionless case considered here corresponds to the limit $\omega \to 0$. In such a case the wavelength of each wave is much greater than the length of the transient domain, $\lambda \gg L$, so that the current speed transition from the left domain $\xi < \xi_1$ to the right domain $\xi > \xi_2$ can be considered as sharp and stepwise. Then using the relationships (see [18])

$${}_2F_1(a,b;b;s) = (1-s)^{-a} \quad \text{and} \quad s\,{}_2F_1(1,1;2;s) = -\ln(1-s),$$

we can calculate functions (19) and (22), as well as (50) and (53), and their derivatives and obtain in the leading order in $\hat{\omega}$ the following asymptotic expressions (bearing in mind that $\zeta = \xi^2$ and $\eta = \xi^{-2}$):

$$
\begin{aligned}
w_2(\zeta) &= -\ln(1-\zeta), & w_2'(\zeta) &= \frac{1}{1-\zeta}, & w_3(\zeta) &= 1, & w_3'(\zeta) &= O(\hat{\omega}^2),\\
\tilde{w}_2(\zeta) &= -\ln(1-\zeta), & \tilde{w}_2'(\zeta) &= \frac{1}{1-\zeta}, & \tilde{w}_3(\zeta) &= 1, & \tilde{w}_3'(\zeta) &= O(\hat{\omega}^2),\\
\breve{w}_1(\eta) &= 1, & \breve{w}_1'(\eta) &= -\frac{\mathrm{i}\hat{\omega}}{2}\frac{1}{1-\eta}, & \breve{w}_3(\eta) &= 1, & \breve{w}_3'(\eta) &= \frac{\mathrm{i}\hat{\omega}}{2\eta},\\
\hat{w}_1(\eta) &= 1, & \hat{w}_1'(\eta) &= \frac{\mathrm{i}\hat{\omega}}{2}\frac{1}{1-\eta}, & \hat{w}_3(\eta) &= 1, & \hat{w}_3'(\eta) &= -\frac{\mathrm{i}\hat{\omega}}{2\eta}.
\end{aligned}
$$

Using these formulae, one can readily calculate the limiting values of transformation coefficients in the long-wave approximation when $\hat{\omega} \to 0$. Their values are presented in the corresponding subsections.

---

[1] W. G. Unruh, "Experimental black-hole evaporation?" Phys. Rev. Lett. **46**, 1351–1353 (1981).

[2] A. Coutant and R. Parentani, "Undulations from amplified low frequency surface waves," Phys. Fluids **26**, 044106 (2014).

[3] S. Robertson, F. Michel, and R. Parentani, "Scattering of gravity waves in subcritical flows over an obstacle," Phys. Rev. D **93**, 124060 (2016).

[4] A. Coutant and S. Weinfurtner, "The imprint of the analogue hawking effect in subcritical flows," Phys. Rev. D **94**, 064026 (2016).

[5] T. G. Philbin, "An exact solution for the hawking effect in a dispersive fluid," Phys. Rev. D **94**, 064053 (2016).

[6] S. Weinfurtner, E. W. Tedford, M. C. J. Penrice, W. G. Unruh, and G. A. Lawrence, "Measurement of stimulated hawking emission in an analogue system," Phys. Rev. Lett. **106**, 021302 (2011).

[7] L.-P. Euvé, F. Michel, R. Parentani, T. G. Philbin, and G. Rousseaux, "Observation of noise correlated by the hawking effect in a water tank," Phys. Rev. Lett. **117**, 121301 (2016).

[8] J. Steinhauer, "Observation of quantum hawking radiation and its entanglement in an analogue black hole," Nat. Phys. **Published online 15 August, doi:10.1038/nphys3863**, 1–7 (2016).

[9] T. Jacobson, "Black hole evaporation and ultrashort distances," Phys. Rev. D **44**, 1731–1739 (1991).

[10] W. G. Unruh, "Sonic analogue of black holes and the effects of high frequencies on black hole evaporation," Phys. Rev. D **51**, 2827–2838 (1995).

[11] D. Faccio, F. Belgiorno, S. Cacciatori, V. Gorini, S. Liberati, and U. Moschella, eds., *Analogue gravity phenomenology*.

[12] L. D. Landau and E. M. Lifshitz, *Fluid Mechanics* (1987).

[13] A. L. Fabrikant and Yu. A. Stepanyants, *Propagation of waves in shear flows* (1998).

[14] P. Maissa, G. Rousseaux, and Y. Stepanyants, "Negative energy waves in shear flow with a linear profile," Eur. J. Mech. – B/Fluids **56**, 192–199 (2016).

[15] S. Churilov, A. Ermakov, G. Rousseaux, and Y. Stepanyants, "Scattering of long water waves in a canal with suddenly changed cross-section in the presence of a current," Phys. Rev. Fluids (to be published). (2017).

[16] R. B. Dingle, *Asymptotic expansions: Their derivation and interpretation* (1973).

[17] F. W. J. Olver, *Introduction to Asymptotics and Special Functions* (1974).

[18] Y. L. Luke, *Mathematical Functions and their Approximations* (1975).

[19] S. Massel, *Hydrodynamics of the Coastal Zone* (1989).

[20] A. Kurkin, S. Semin, and Y. Stepanyants, "Surface water waves transformation over a bottom ledge," Izv. Atmos. Ocean. Phys. **50**, 29–35 (2015).

[21] I. S. Gradshteyn and I. M. Ryzhik, *Table of integrals, series, and products*, 7th ed. (Academic Press, Amsterdam et al., 2007).

[22] S. Robertson and R. Parentani, "Hawking radiation in the presence of high-momentum dissipation," Phys. Rev. D **92**, 044043 (2015).

[23] J. Adamek, X. Busch, and R. Parentani, "Dissipative fields in de sitter and black hole spacetimes: quantum entanglement due to pair production and dissipation," Phys. Rev. D **87**, 124039 (2013).